

# Development of Silicon Drift Detectors and recent applications\*

\*a personal view

(dedicated to Pavel Rehak - 1945-2009)

Chiara Guazzoni

Politecnico di Milano and INFN Sezione di Milano

e-mail: [Chiara.Guazzoni@mi.infn.it](mailto:Chiara.Guazzoni@mi.infn.it)

[home.deib.polimi.it/guazzoni](http://home.deib.polimi.it/guazzoni)

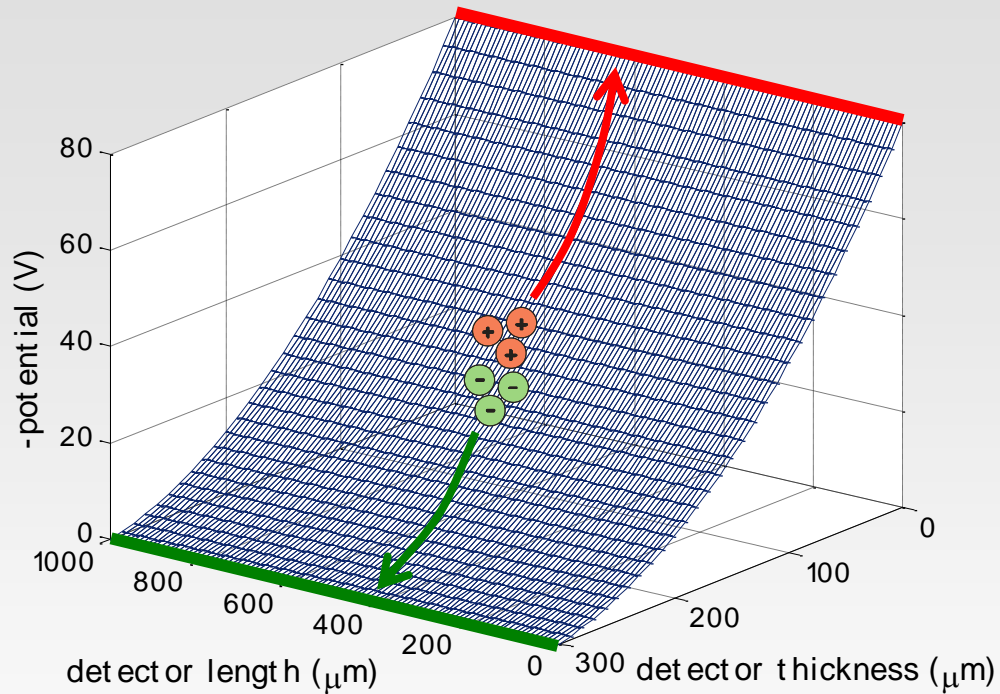
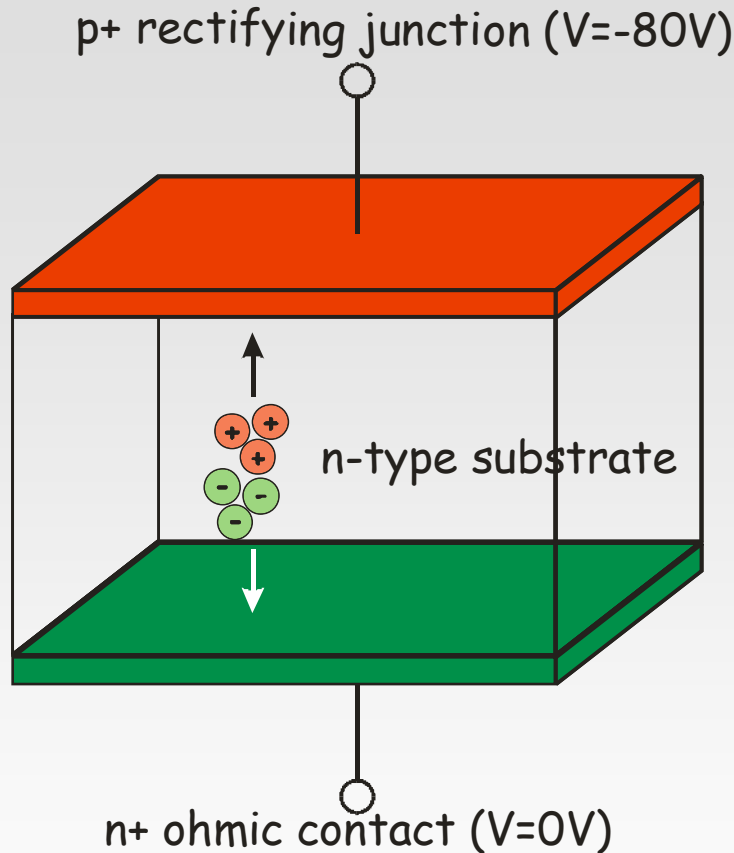
# Outline

- ✧ The idea of sideways depletion
- ✧ Optimized SDD Topologies
  - spectroscopy
  - 2D position sensing
- ✧ Evolution towards spectroscopic imaging: MLSDD and CDD
- ✧ Outlook to applications:
  - X-Ray Fluorescence and Proton Induced X-Ray Emission
  - Gamma-ray imaging
  - Advanced X-ray imaging modalities
  - Macro-pixel arrays with DEPFET readout for XFEL

## ✧ Conclusions



# Planar pn diodes

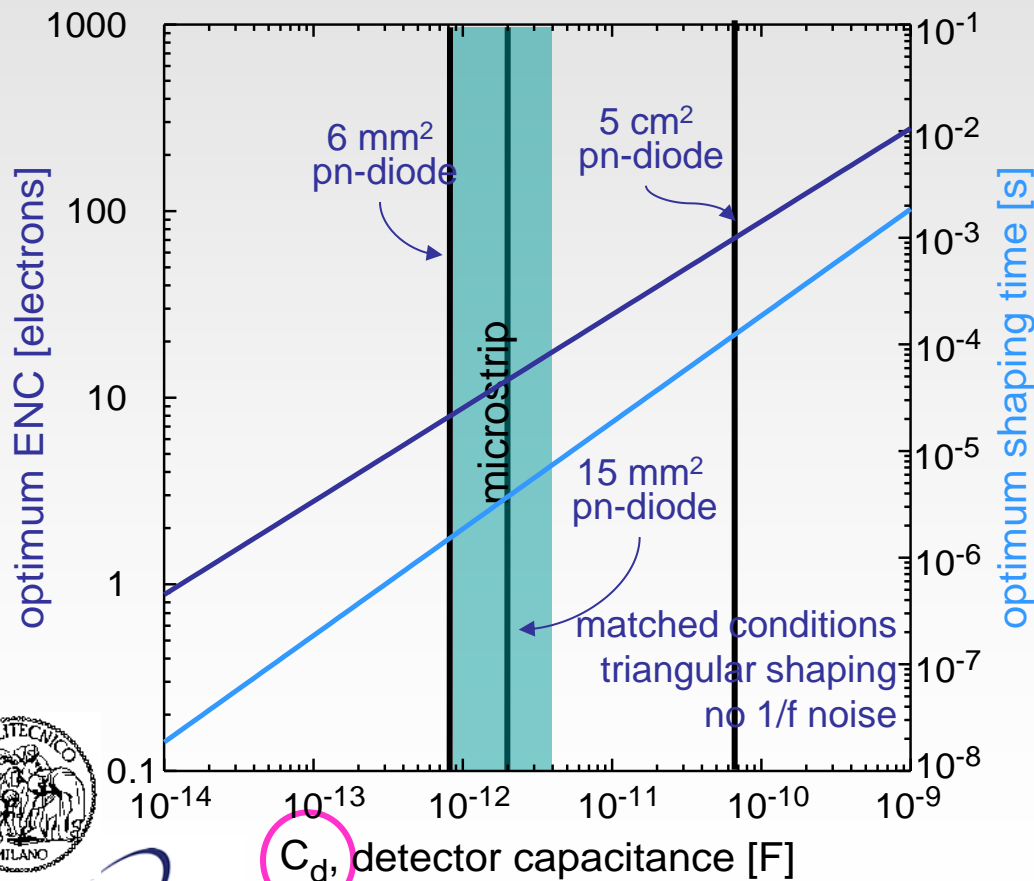


- Detector capacitance increases with diode active area
- Detector capacitance decreases if diode thickness is increased



# Planar pn diodes

$$ENC_{opt}^2 = \underbrace{\sqrt{A_1 A_3} \sqrt{2kTq} \sqrt{\frac{\alpha}{\omega_T}}}_{FET} \underbrace{\sqrt{C_d I_L}}_{detector} \underbrace{\left( \sqrt{\frac{C_G}{C_d}} + \sqrt{\frac{C_d}{C_G}} \right)}_{matching} + ENC_{1/f}^2 (C_T^2)$$



$$\tau_{opt} = \sqrt{\frac{A_1}{A_3}} \sqrt{2V_{th}} \underbrace{\sqrt{\frac{\alpha}{\omega_T}}}_{FET} \underbrace{\sqrt{\frac{C_d}{I_L}}}_{detector}$$

$$\underbrace{\left( \sqrt{\frac{C_G}{C_d}} + \sqrt{\frac{C_d}{C_G}} \right)}_{matching} = \sqrt{\frac{A_1}{A_3}} \tau_c$$

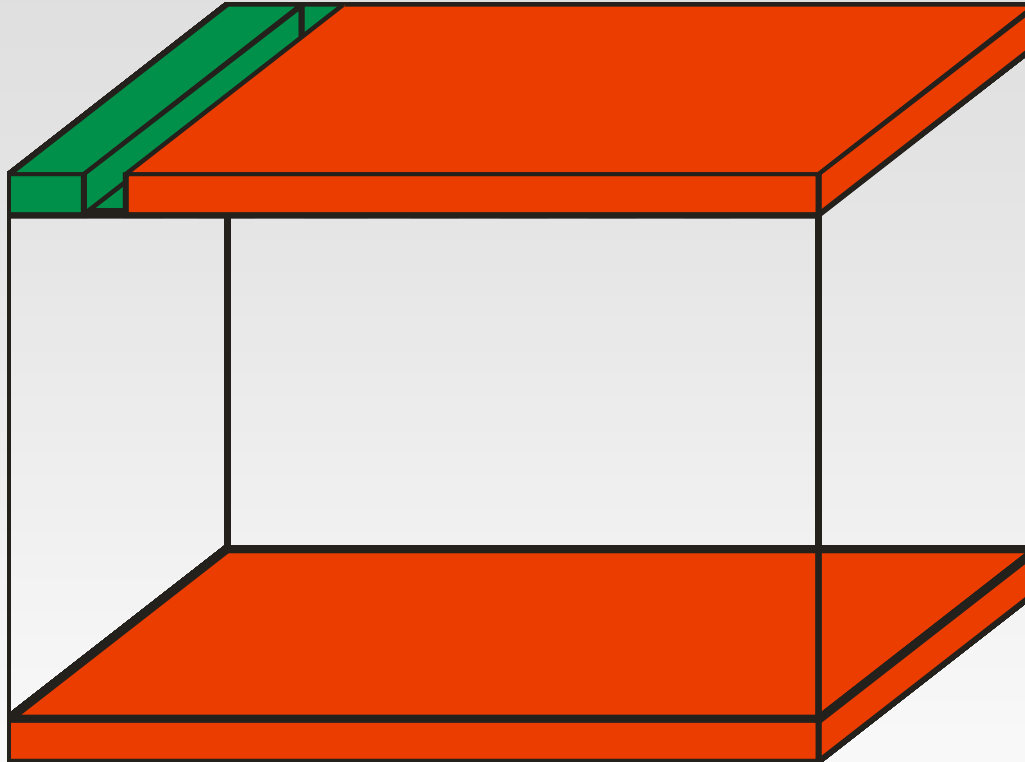
Energy resolution  
&  
Count rate capability  
require

**capacitance minimization**



# The sideward depletion

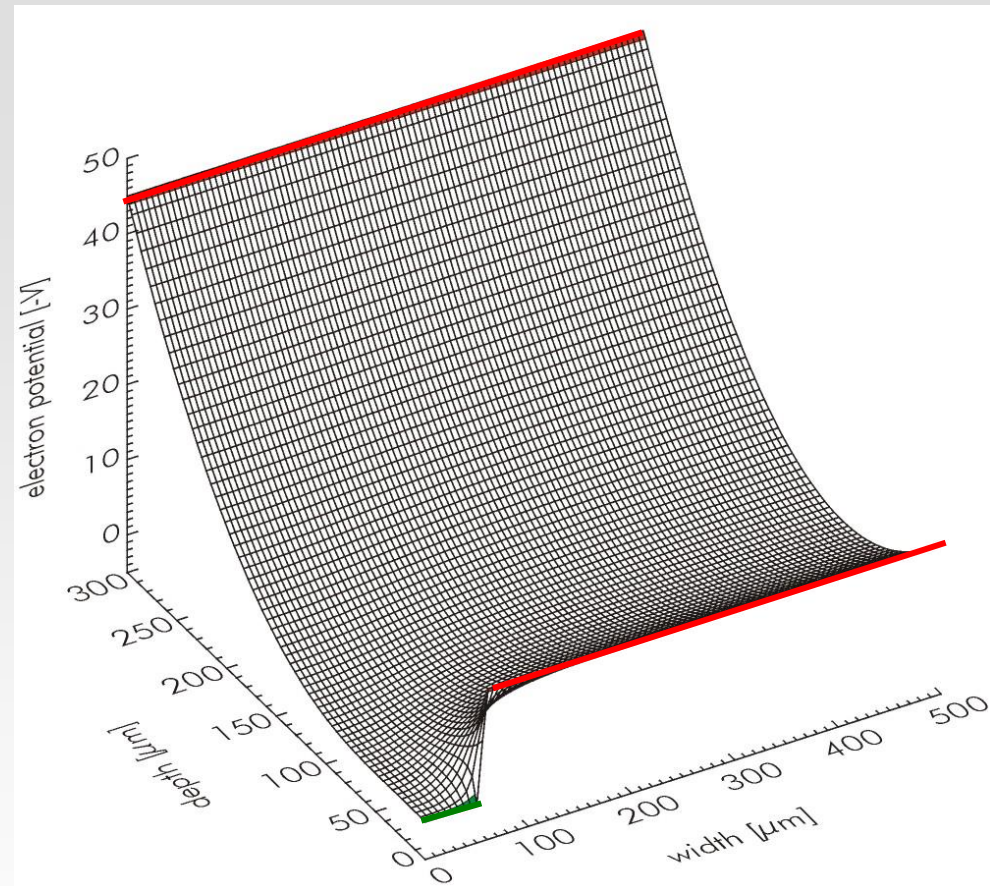
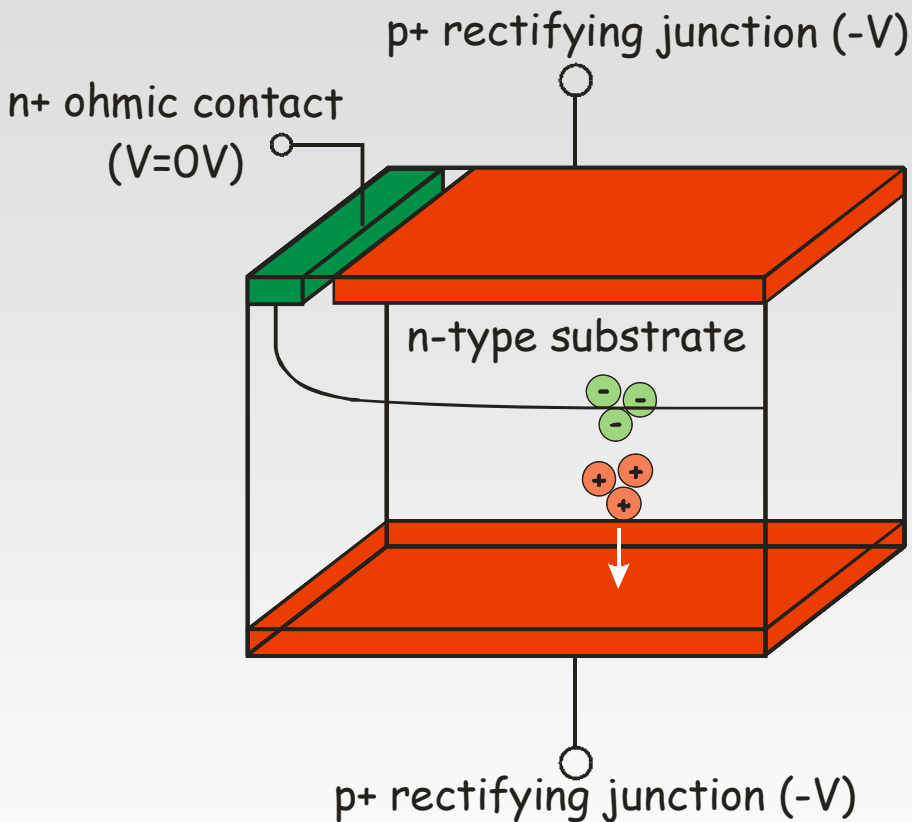
Emilio Gatti & Pavel Rehak, Autumn 1982



basic idea of sideward depletion — the revolutionary concept at the heart of the Silicon Drift Detector — is to fully deplete the semiconductor substrate through a pointlike “virtual contact,” as it is called in Gatti and Rehak’s original paper.



# The sideward depletion

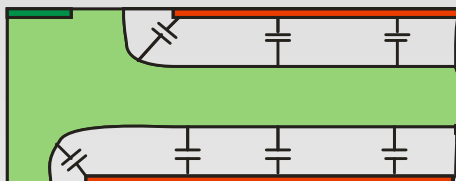


- Detector volume fully depleted by "virtual contact" (point-like)
- Full depletion achieved with only a quarter of the bias necessary for standard p-n diodes

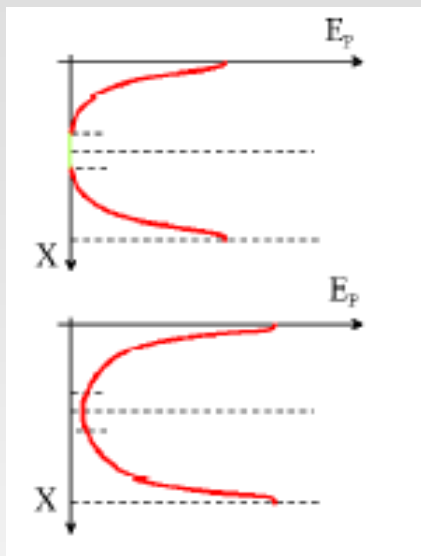


# The sideward depletion

## Below depletion



## At full depletion



## Impact on anode capacitance

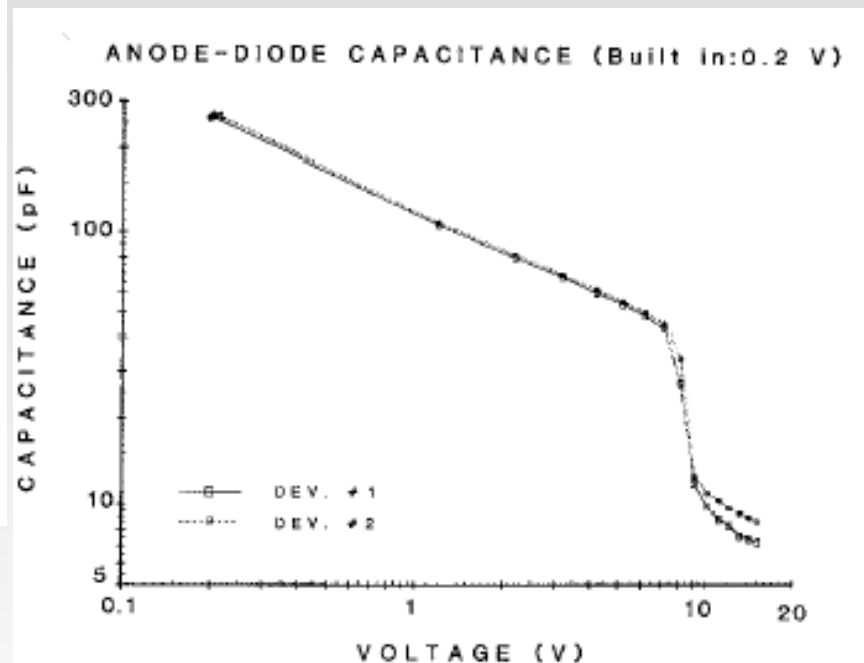


Fig. 12. Capacitance versus voltage plots of two of the test devices provided on the wafer for monitoring its doping uniformity.

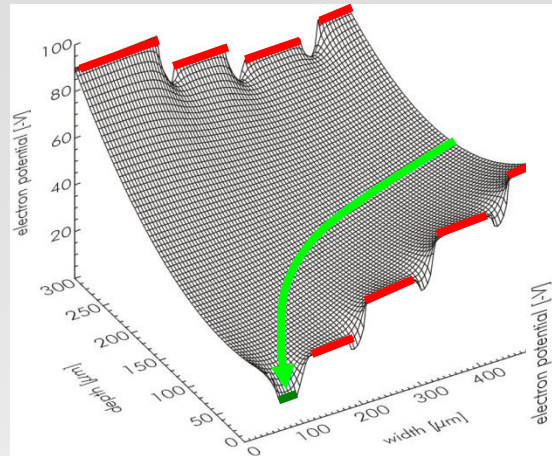
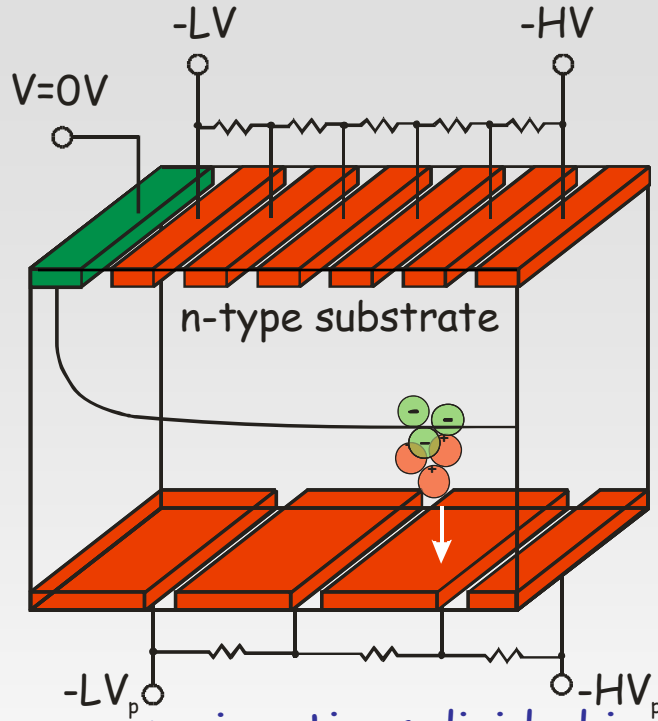
- At nearly full depletion the conductive channel at the middle of the detector retracts causing the capacitance to drop abruptly.

- At higher bias voltages the remaining capacitance is the lowest capacitance between the  $n^+$  contact and the  $p^+$  electrodes.



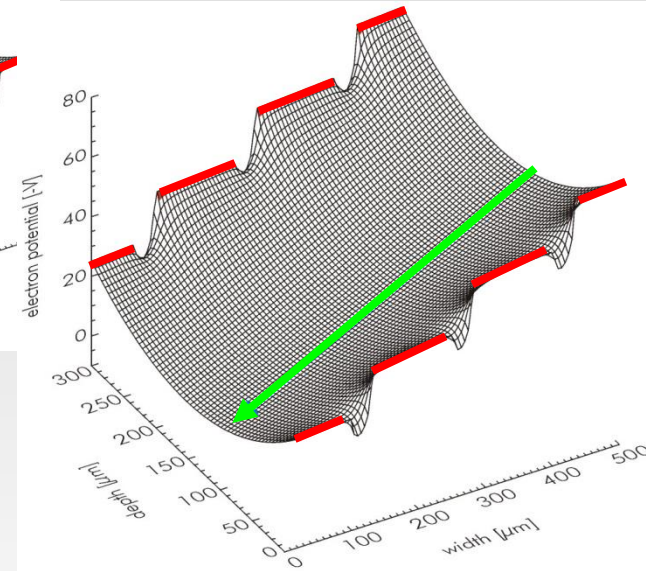


# Silicon Drift Detector



Near the anode...

Central drift region...



- p+ junctions divided in strips with increasing potential on both sides → nearly uniform drift field parallel to the surface
- signal electrons focused in the center of the wafer transported at constant velocity towards the readout anode
- 1-D position sensing with only 1 readout channel through drift time
- small anode capacitance → low-noise measurement of time and amplitude





# 1984: Patent filed...

**United States Patent** [19]

**Rehak et al.**

[11] **Patent Number:** 4,688,067

[45] **Date of Patent:** Aug. 18, 1987

[54] **CARRIER TRANSPORT AND COLLECTION IN FULLY DEPLETED SEMICONDUCTORS BY A COMBINED ACTION OF THE SPACE CHARGE FIELD AND THE FIELD DUE TO ELECTRODE VOLTAGES**

[75] **Inventors:** Pavel Rehak, Patchogue, N.Y.;  
Emilio Gatti, Lesmo, Italy

[73] **Assignee:** The United States of America as  
represented by the Department of  
Energy, Washington, D.C.

[21] **Appl. No.:** 583,553

[22] **Filed:** Feb. 24, 1984

## FOREIGN PATENT DOCUMENTS

974659 9/1975 Canada ..... 357/24 M

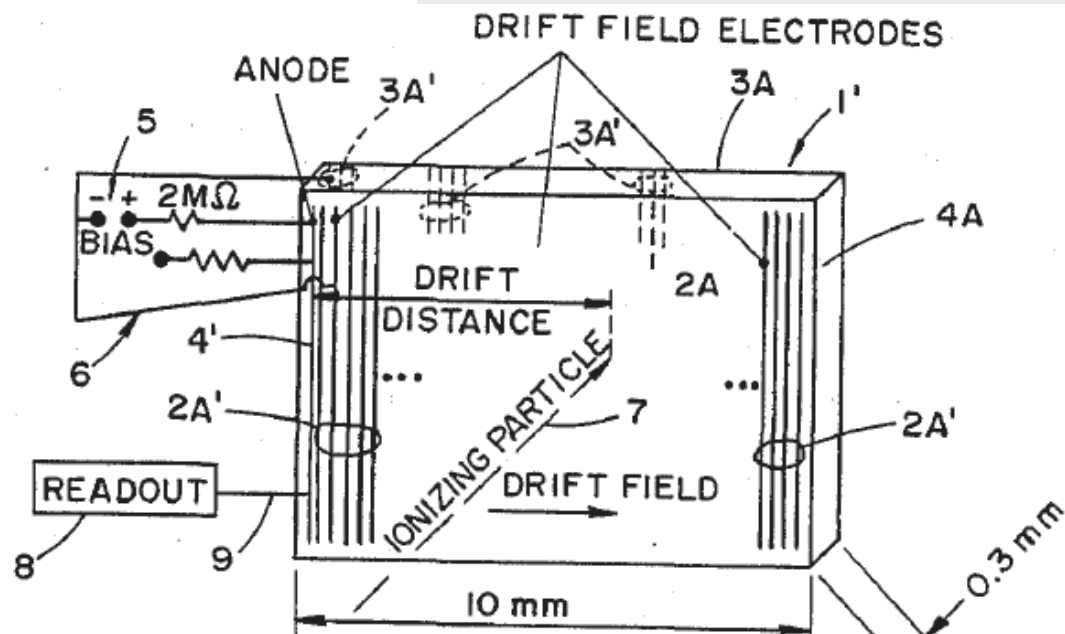
## OTHER PUBLICATIONS

Gatti et al, "The Concept of a Solid State Drift Chamber" DPF Workshop Collider Detectors, Lawrence Berkeley Lab., Feb. 28-Mar. 4, 1983.

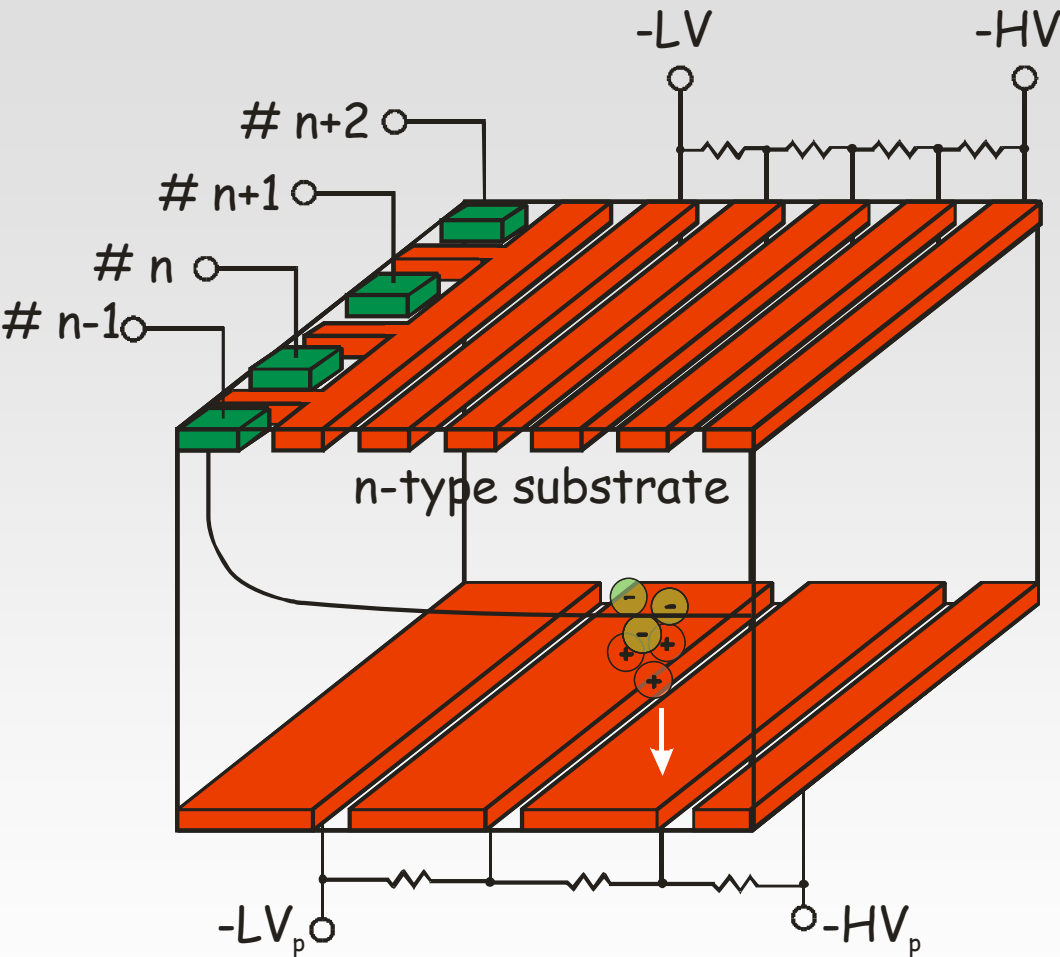
Gatti et al, "Semiconductor Drift Chamber . . ." 2nd Pisa Meeting on Advanced Detectors, Grosseto, Italy, Jun. 3-7, 1983.

*Primary Examiner*  
*Attorney, Agent,*  
*Gottlieb; Judsor*

[57]



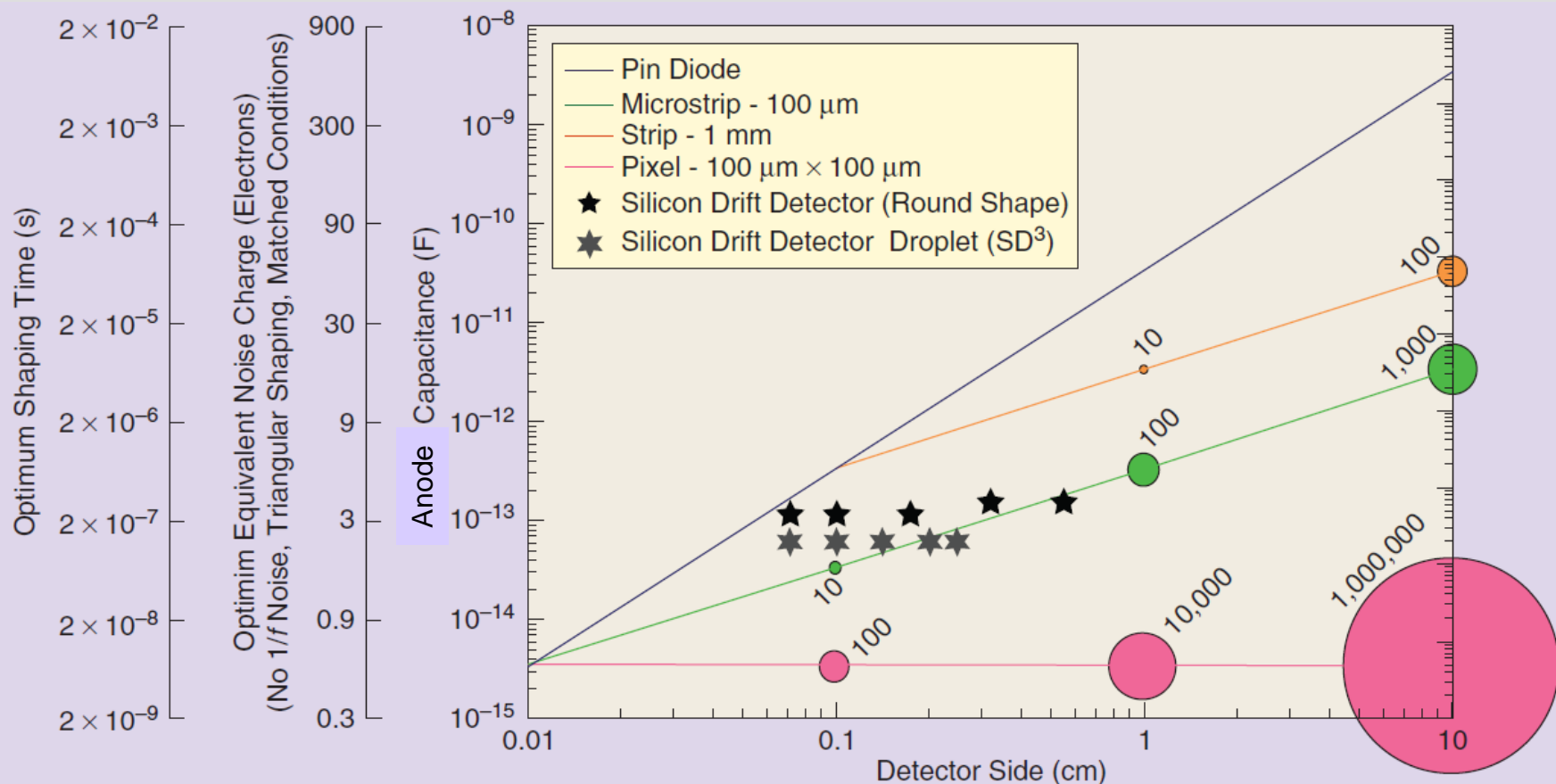
# Multianode Silicon Drift Detectors



- granularity of the anodes provides lateral interaction coordinate
- drift time measurement gives position along drift coordinate with high resolution:
  - $\sim 2\mu\text{m}$  in lab,
  - $\sim 10\mu\text{m}$  in test beam
  - $\sim 20\mu\text{m}$  in experiments
- external trigger required for 2D position sensing



# The Silicon Drift Detector break-through



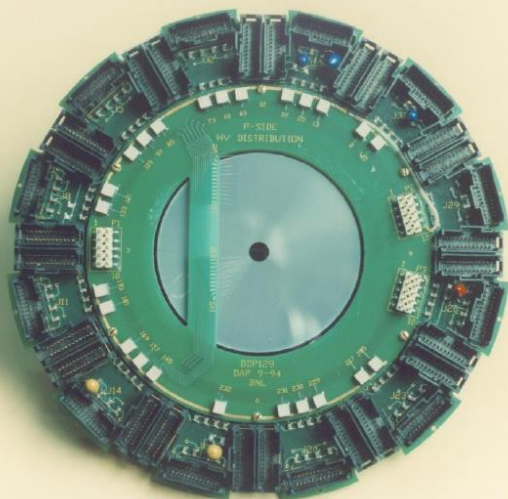
Anode capacitance (of a 300- $\mu\text{m}$ -thick silicon detector), achievable optimal ENC, and optimal shaping time, in the case of no 1/f noise and of triangular shaping for matched conditions between the detector capacitance and the front-end electronics input capacitance, as a function of detector side length for different detector families. The stars report the corresponding values for silicon drift detectors (SDDs) for X-ray spectroscopy. Due to their circular shape, as side length we considered the radius of the active area. This shows how detectors based on the sideward depletion principle broke the tie between active area and output capacitance. The bubble chart represents the number of detector channels needed for a given active area.



# SDDs in High Energy Physics

## NA45 - CERES

@ CERN's LEP (1992-2000)



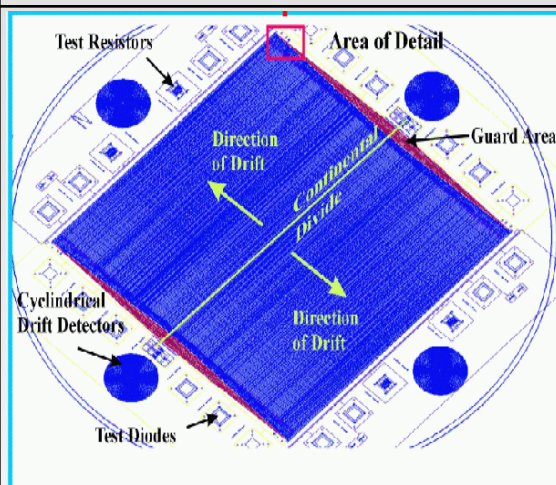
**Wafer:** 1<sup>st</sup> ver.: 3" Silicon,  
280  $\mu\text{m}$  thick  
2<sup>nd</sup> ver.: 4" Silicon

**Active area:** 32  $\text{cm}^2$ /55  $\text{cm}^2$   
360 collecting anodes

**Foundry:** BNL/Sintef

## STAR

@ BNL RHIC (install Feb.01)



**Wafer:** 4" (NTD) Silicon,  
3  $\text{k}\Omega\text{cm}$  resistivity,  
280  $\mu\text{m}$  thick

**Active area:** 6.3  $\times$  6.3  $\text{cm}^2$   
2  $\times$  240 collecting anodes

**Foundry:** Sintef

## ALICE

@ CERN's LHC



**Wafer:** 5" (NTD) Silicon,  
3  $\text{k}\Omega\text{cm}$  resistivity,  
300  $\mu\text{m}$  thick

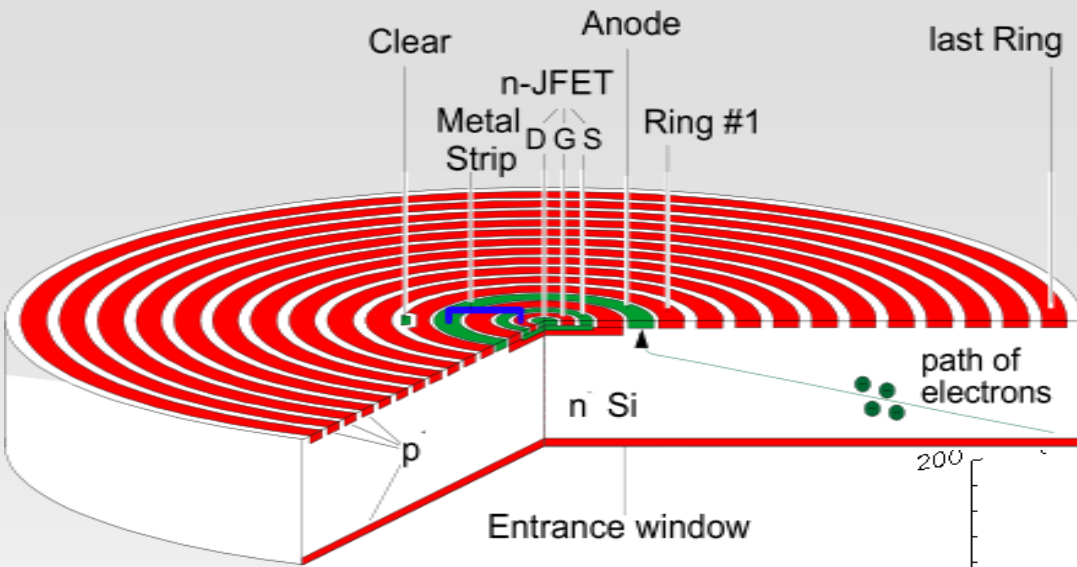
**Active area:** 7.02  $\times$  7.53  $\text{cm}^2$   
512 collecting anodes

**Foundry:** Canberra



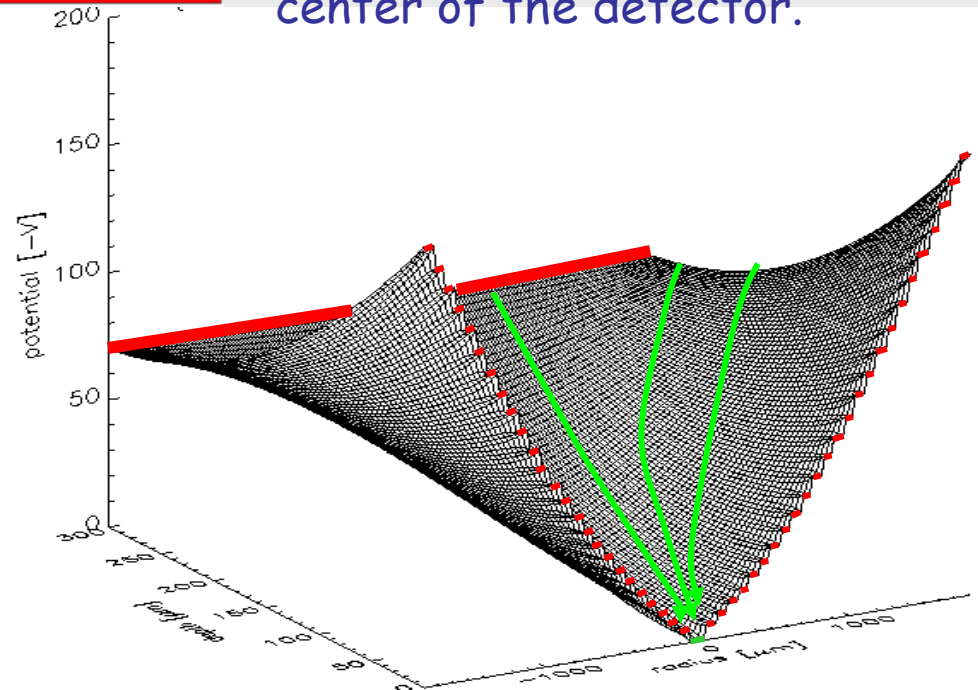


# SDD for high resolution X-ray spectroscopy



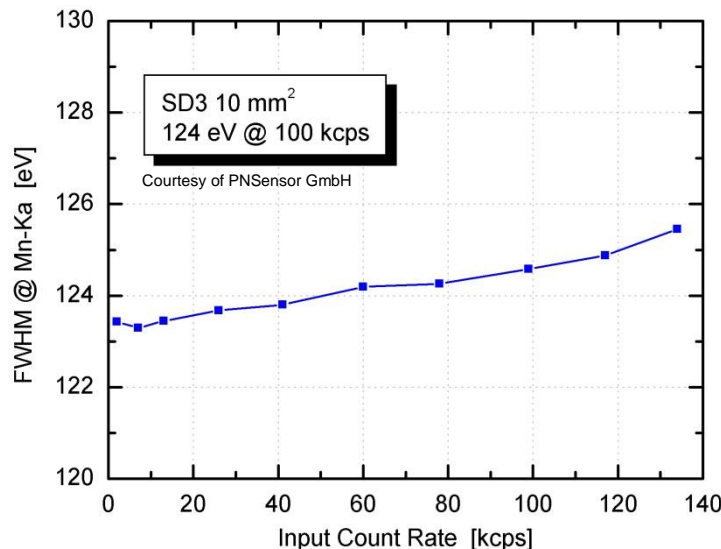
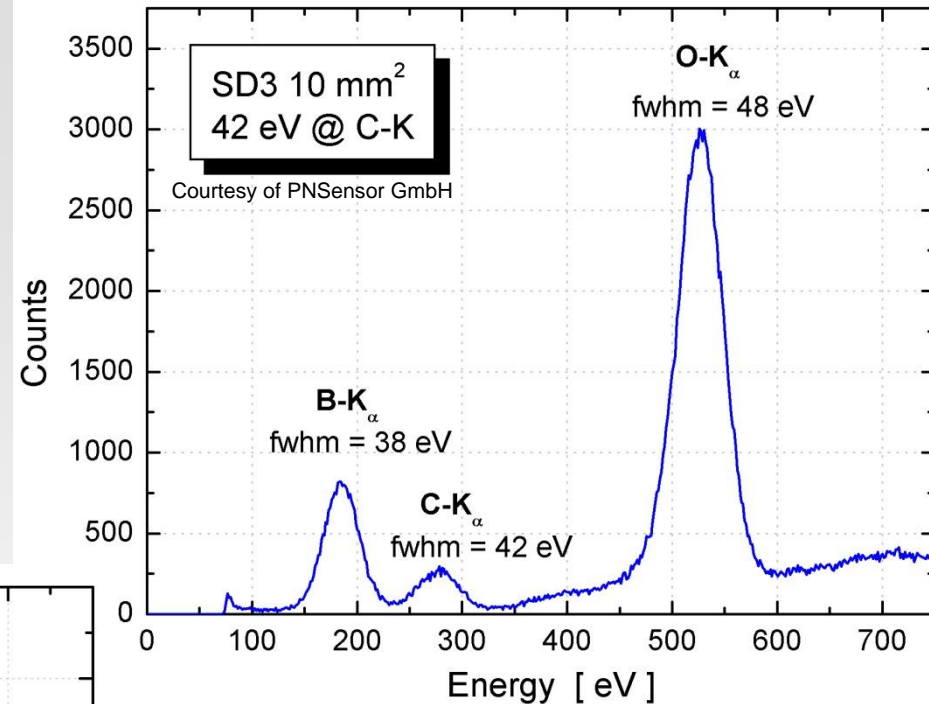
- continuous p+ back contact acting as entrance window
- cylindrical geometry with anode in the center
- transistor located in the center of the detector.

- drift field azimuthally symmetric
- electrons produced anywhere within detector active area are collected at the central anode
- detector capacitance  $\cong 100$  fF



# SDDs for high res. spectroscopy

- Anode capacitance:  $\sim 200$  fF
- Energy resolution:  $\Delta E_{FWHM} = 125$  eV (equivalent to  $ENC=4$  el. r.m.s.) @ 200kcps
- Count rate capability: up to  $10^6$  cps
- Peak/Background  $\approx 10.000 : 1$
- Quantum efficiency:  $> 90\%$  @ 0.3-10 keV (Boron line detection)
- Rad. hardness:  $> 10^{14}$   $Mo_K$  photons
- Operating temperature:  $T \approx -10^\circ C$

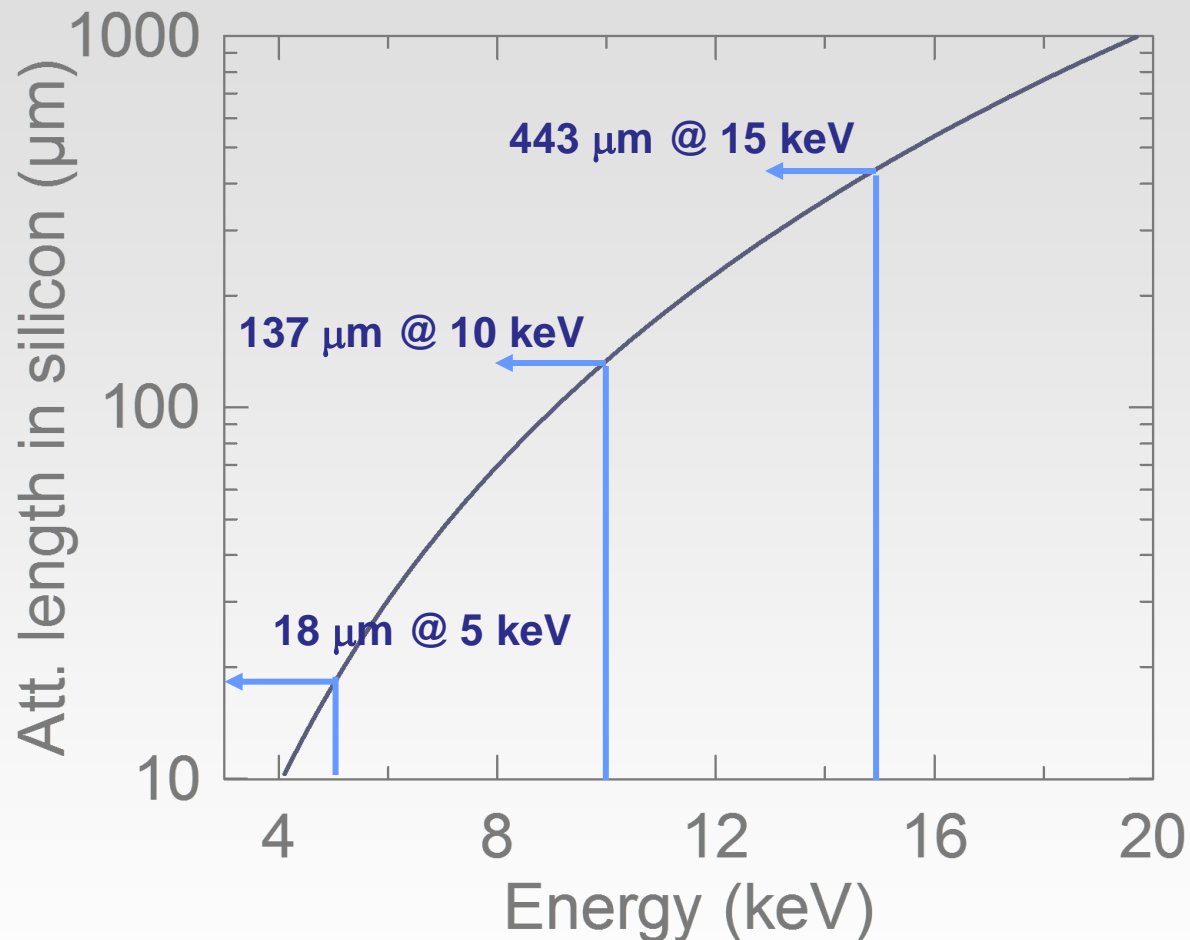


with pulset reset PA thanks to  
on-chip reset diode

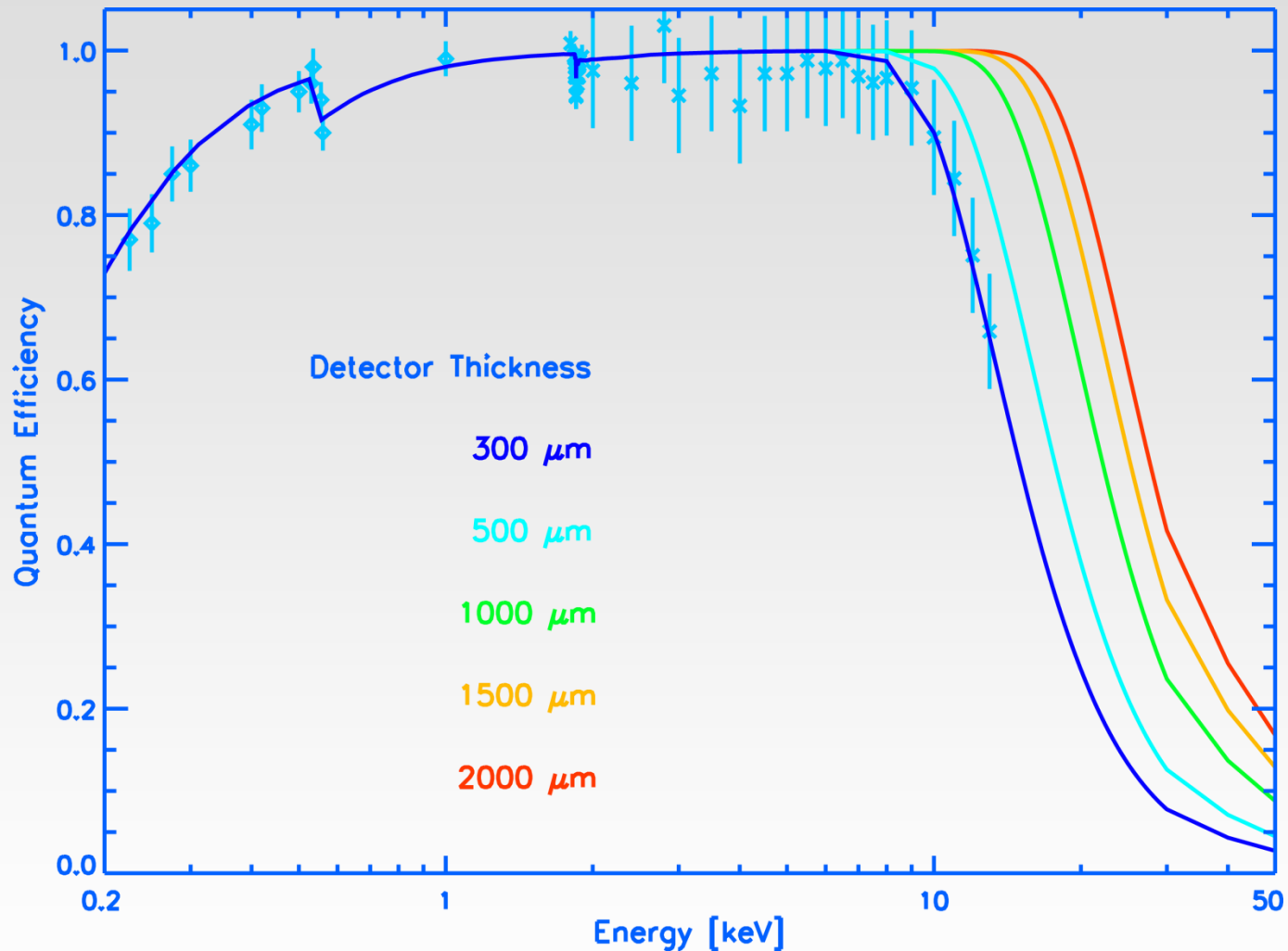




# Silicon quantum efficiency

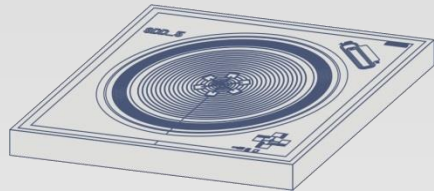


# Silicon quantum efficiency



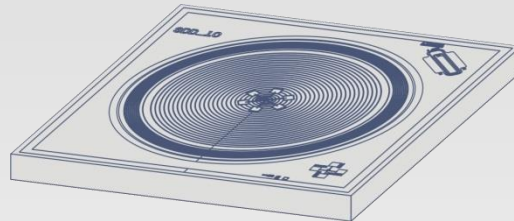
# SDDs for high res. spectroscopy

Commercially available classic cylindrical SDDs with sensitive area of 5, 10 and 20 and 30 mm<sup>2</sup> up to 1cm<sup>2</sup>



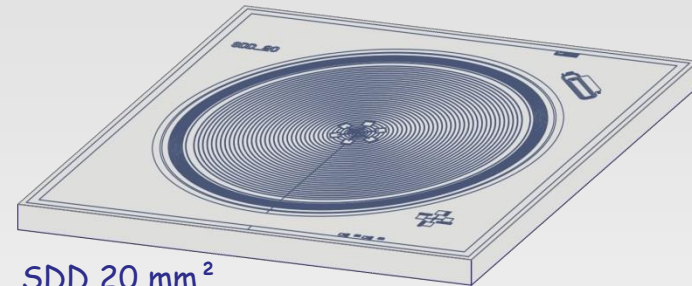
SDD 5 mm<sup>2</sup>

chip 5 × 5 × 0.45 mm<sup>3</sup>



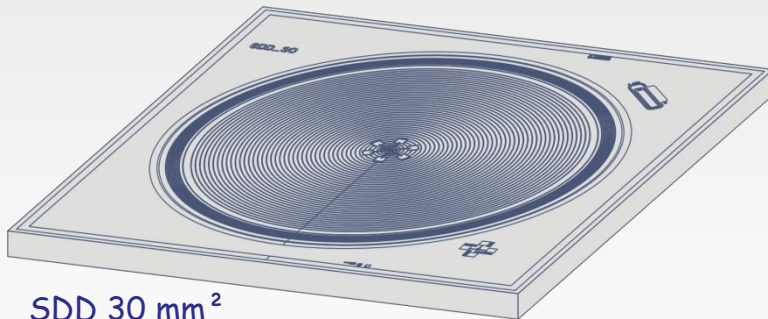
SDD 10 mm<sup>2</sup>

chip 6 × 6 × 0.45 mm<sup>3</sup>



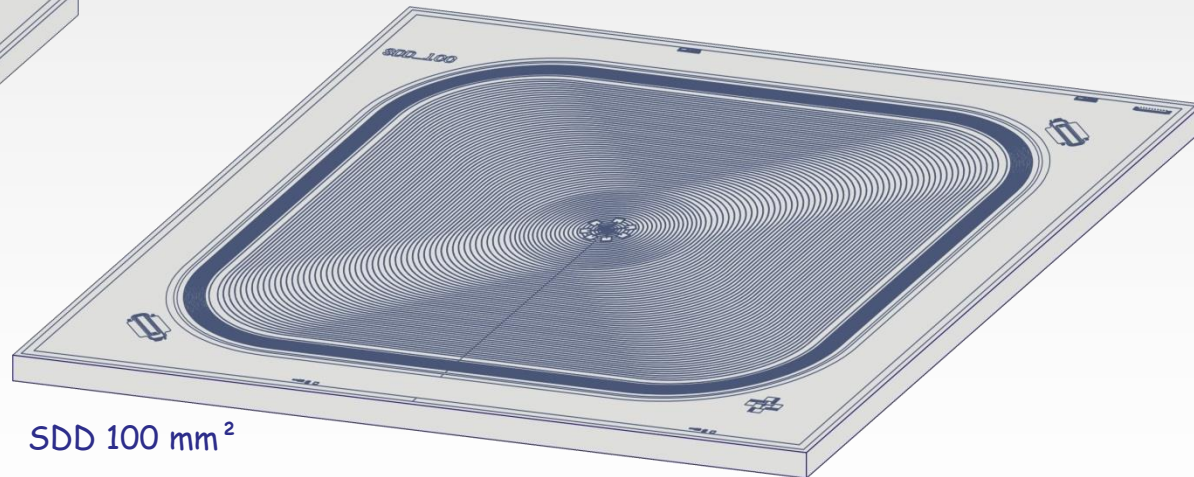
SDD 20 mm<sup>2</sup>

chip 8 × 8 × 0.45 mm<sup>3</sup>



SDD 30 mm<sup>2</sup>

chip 9 × 9 × 0.45 mm<sup>3</sup>

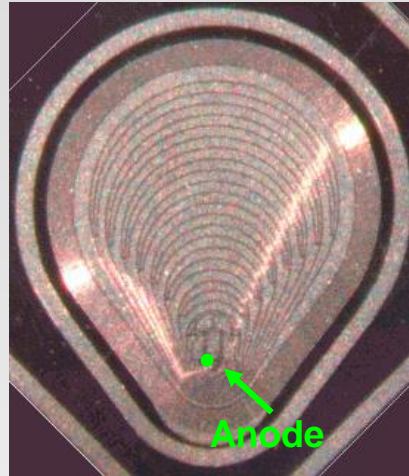
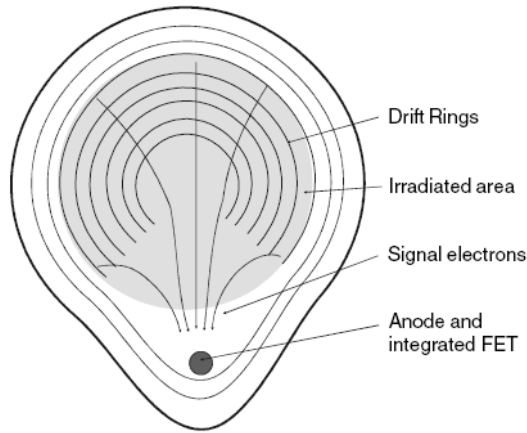


SDD 100 mm<sup>2</sup>

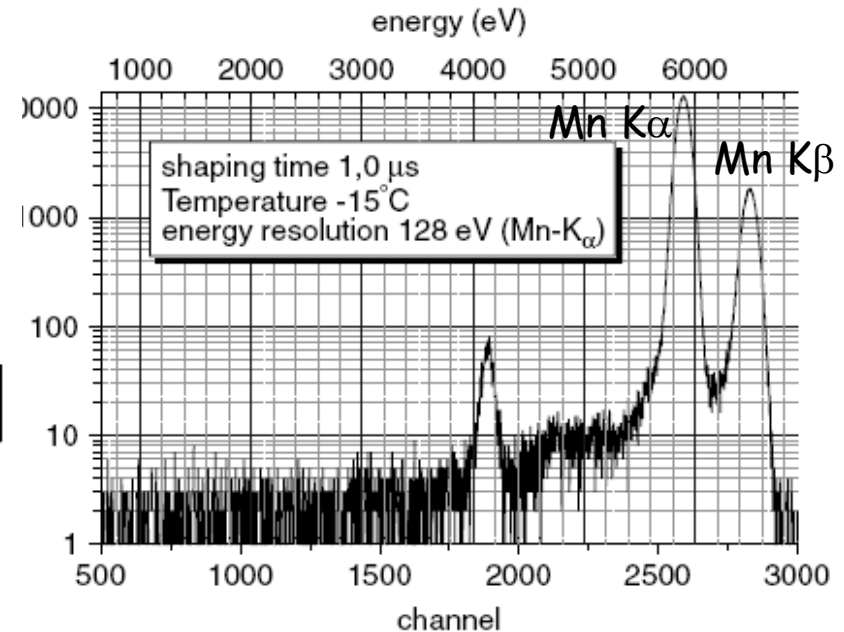
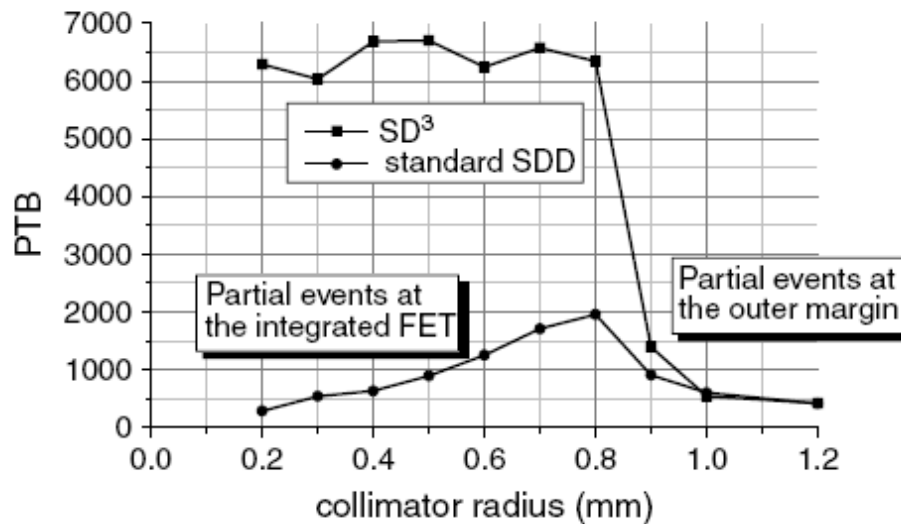
chip 14 × 14 × 0.45 mm<sup>3</sup>



# Droplet SDDs: novel evolution

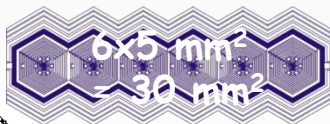
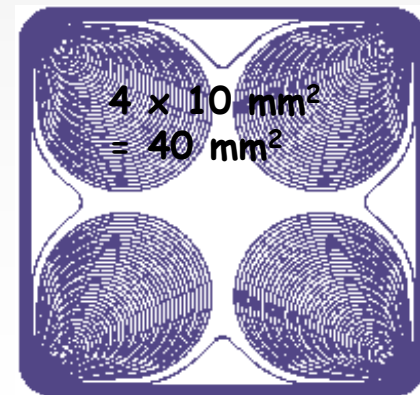
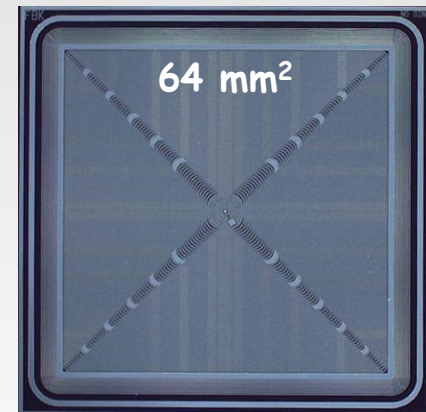
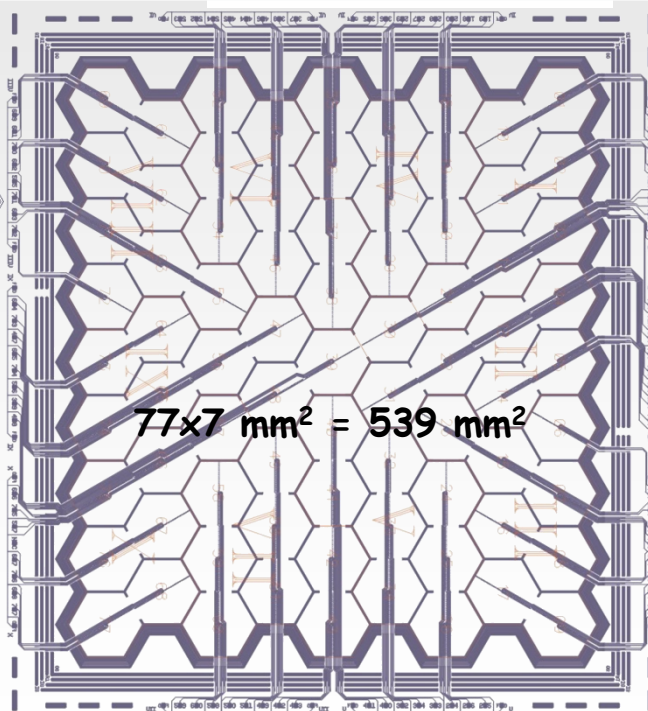
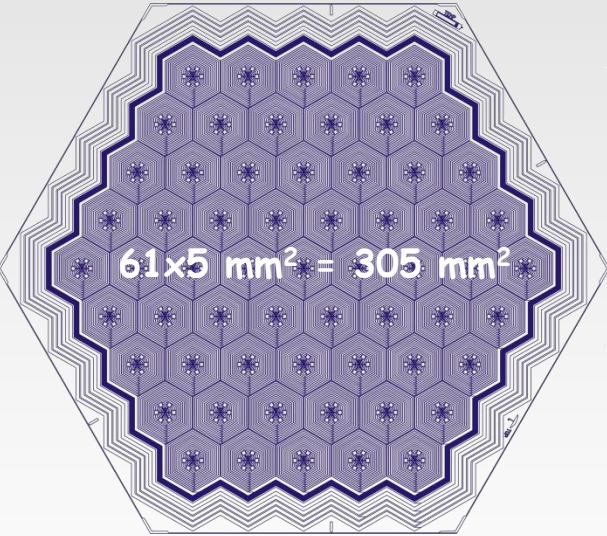
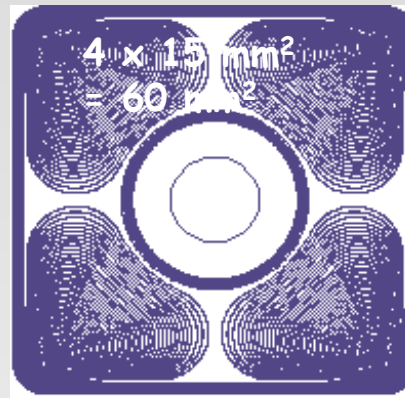
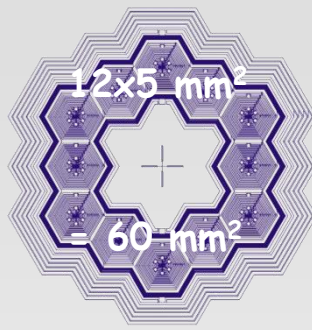
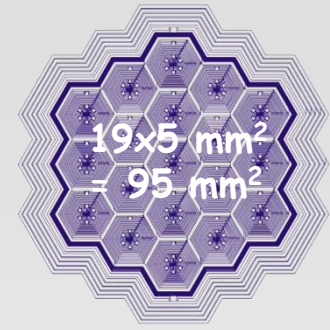
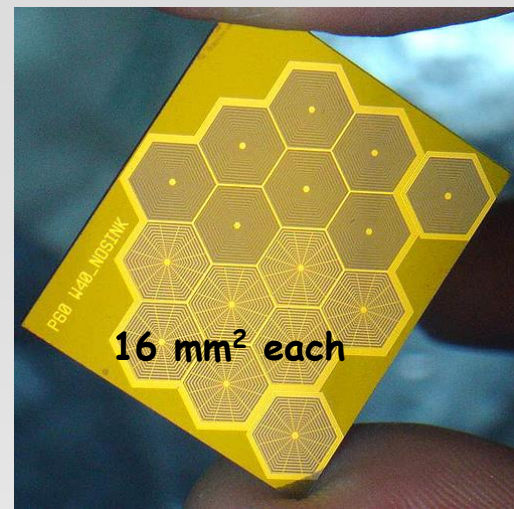


- Anode + on-chip JFET outside detector active area → improvement of the peak-to-background ratio.
- Very small collecting anode → output capacitance about 120 fF much lower than conventional SDDs (larger than 200 fF)



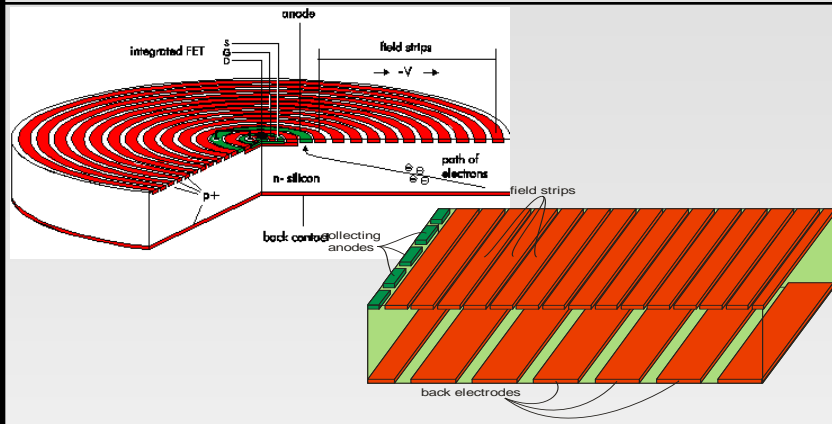


# Multichannel SDDs

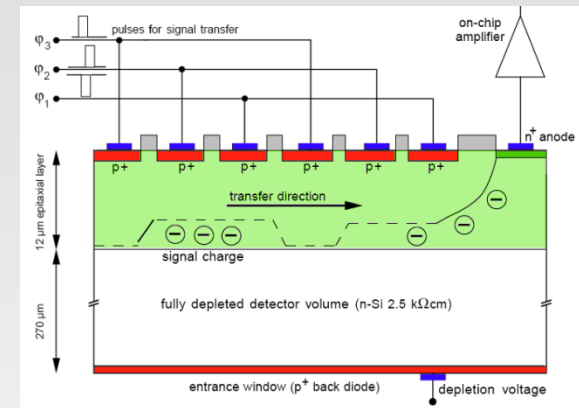


# Sideward Depletion Family Tree

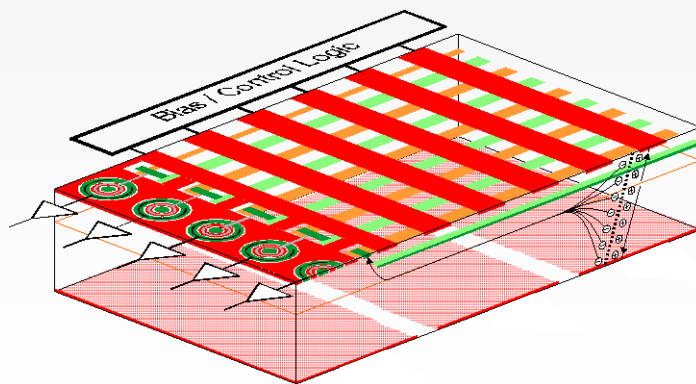
## Silicon Drift Detector



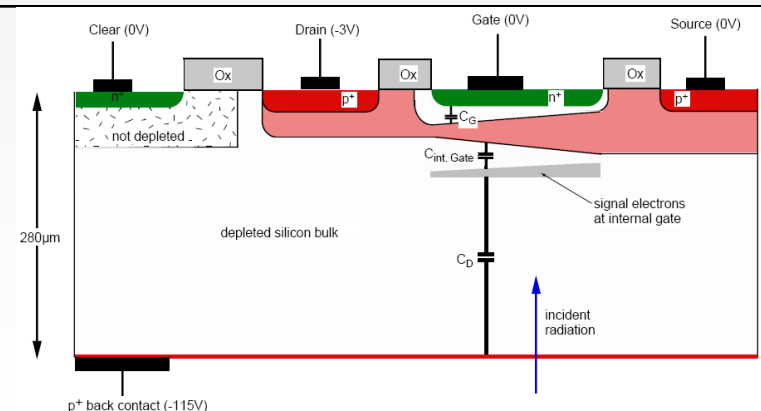
## Fully Depleted pnCCD



## Controlled-Drift Detector

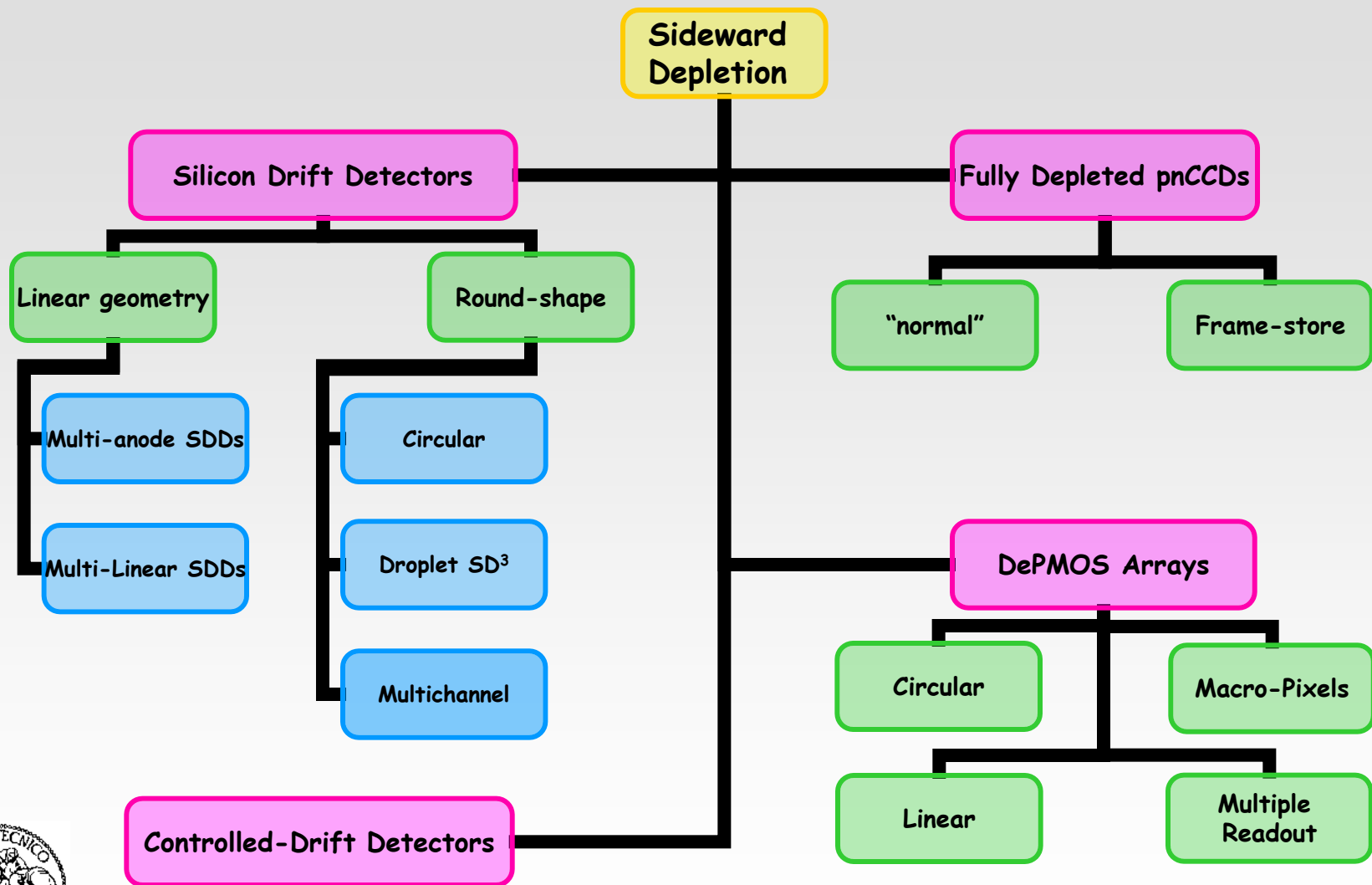


## DePMOS





# Sideward Depletion Family Tree



# Limitations of SDD for 2D position sensing

## ➤ START TRIGGER NEEDED !

no imaging of random sources ( $x/\gamma/\dots$ ) !

## ➤ FREE LATERAL BROADENING

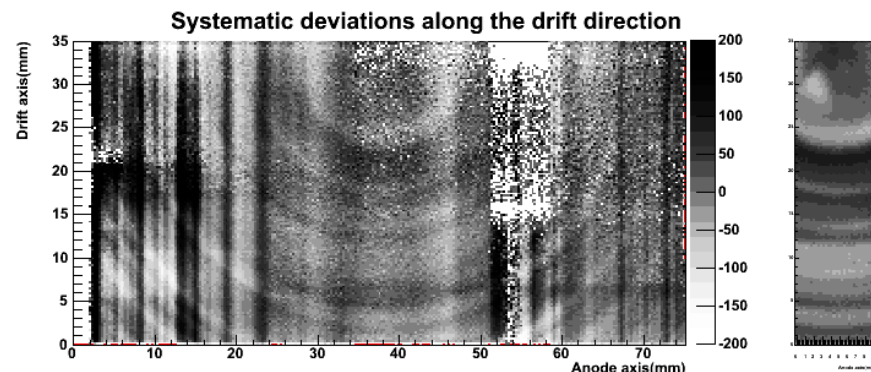
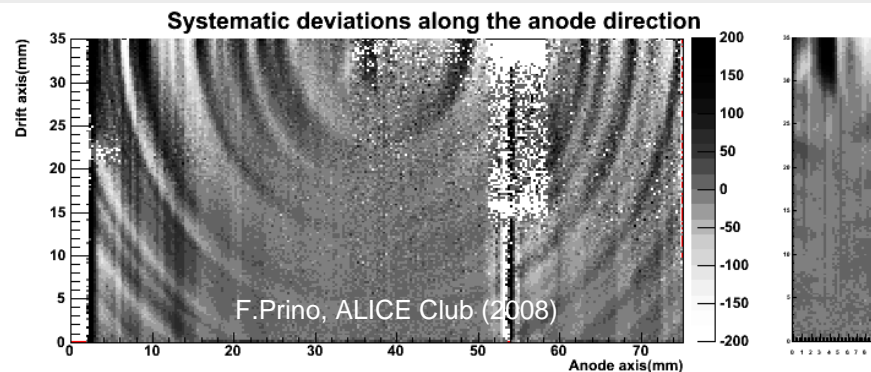
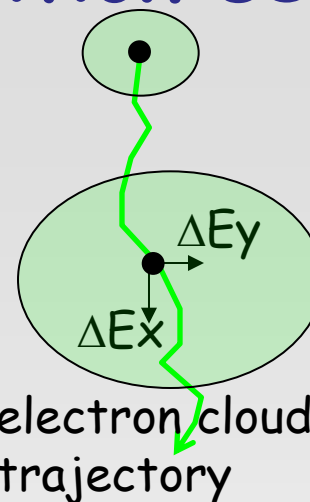
😊 position resolution along anodes improved by interpolation

😞 centroid algorithm not optimal for all incident positions

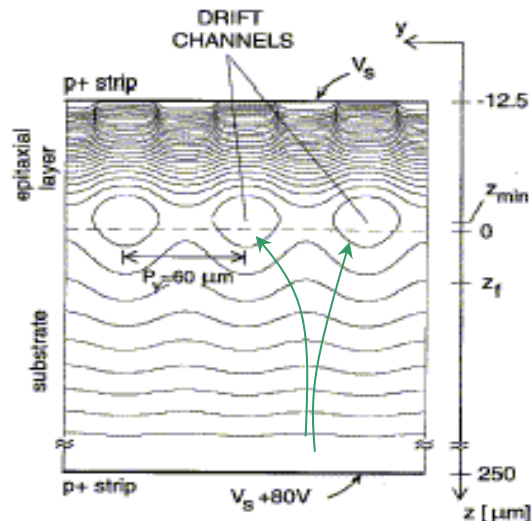
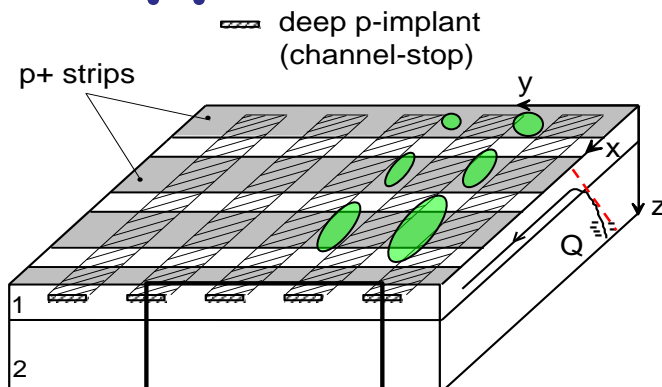
😞 charge sharing limits spectroscopic performance and reduces event rate

## ➤ DOPING INHOMOGENEITIES

😞 systematic deviations (up to  $\pm 200\mu\text{m}$ ) along anode direction

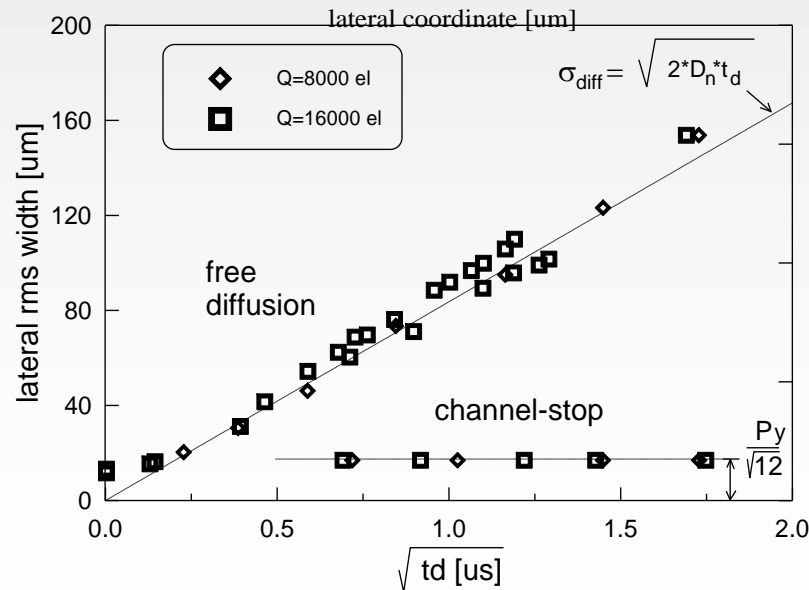
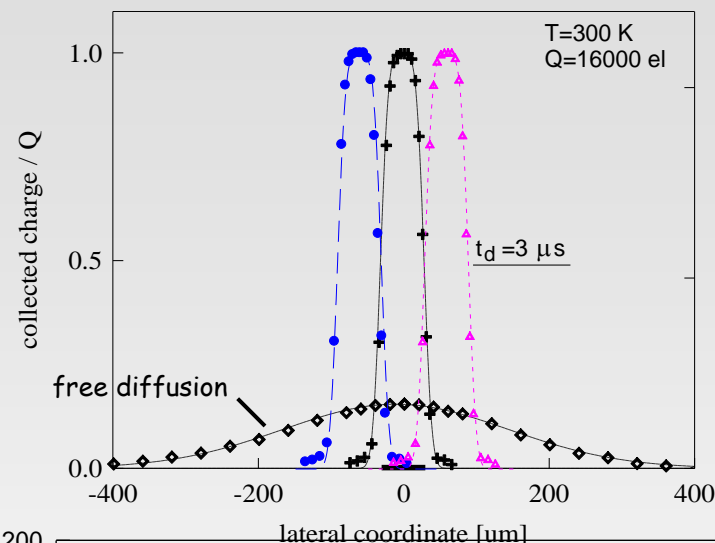


# Suppression of lateral broadening

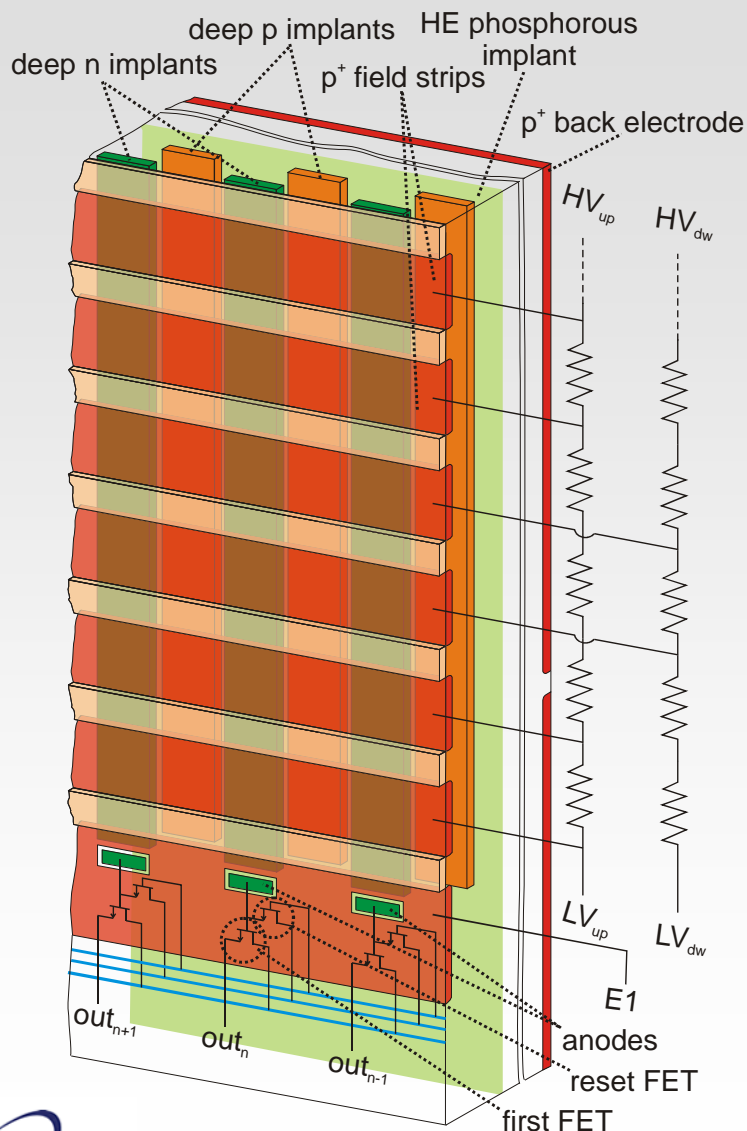


- cloud size independent of interaction point
- compensation of doping inhomogeneities
- high count rate applications
- event timing via signal induction

A.Castoldi, P.Rehak, P.Holl, "A New Silicon Drift Detector With Reduced Lateral Diffusion" Nucl. Instr. and Meth., A377 (1996) 375-380.



# Multi-Linear SDD architecture



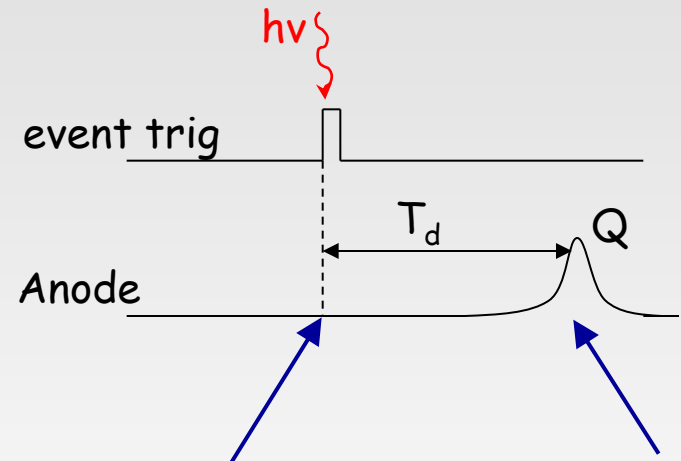
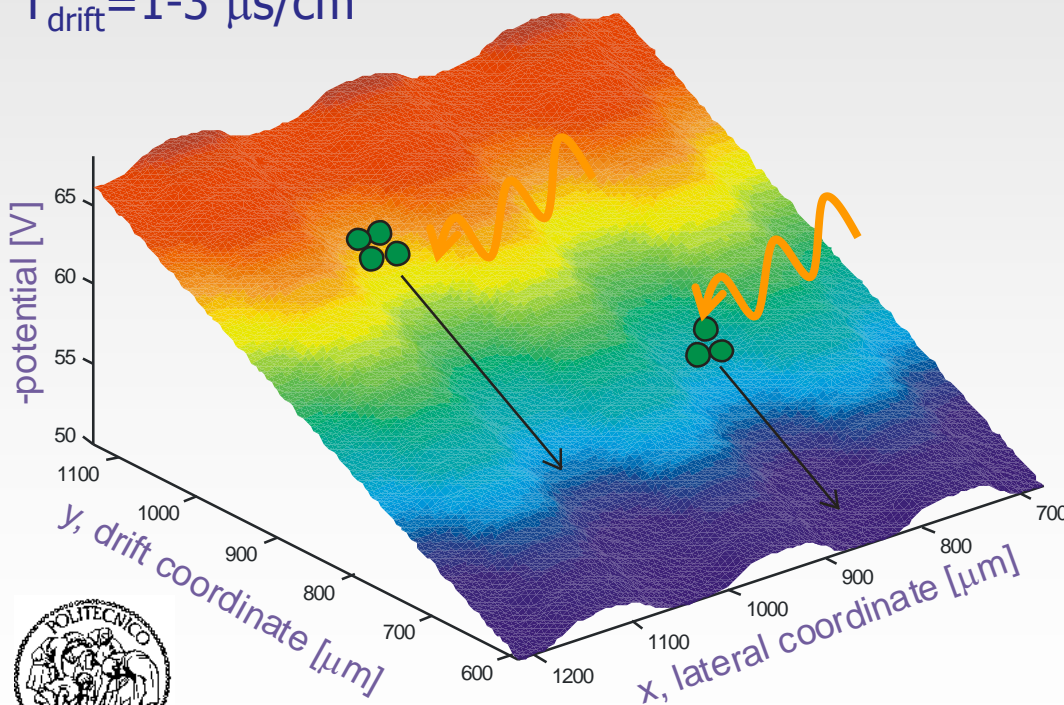
- ✦ fully depleted n-type bulk
- ✦ p+ entrance window implanted on the back side
- ✦ array of p+ strips implanted on the front side
- ✦ **channel-stops (deep p-implants)** for lateral confinement
- ✦ **channel-guides (deep n-implants)** for lateral confinement and drift enhancement
- ✦ HE n implant locates the drift channel close to the finely structured surface
- ✦ on-chip electronics (JFET in source follower configuration)



# MLSDD operating modalities - I

- free-running mode (external trigger)
- free-running mode (self-trigger from back side)

$T_{\text{drift}} = 1-3 \mu\text{s/cm}$



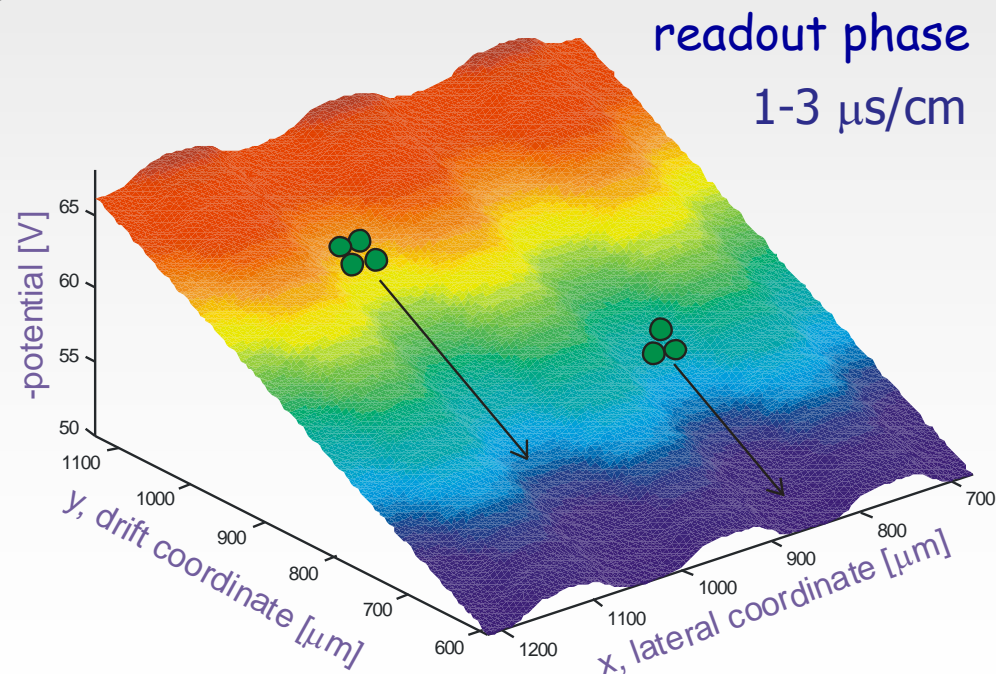
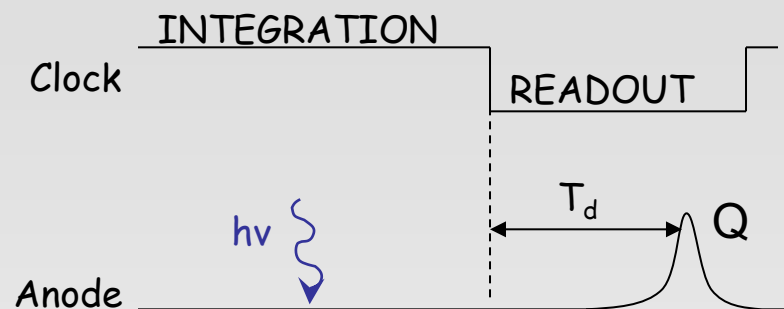
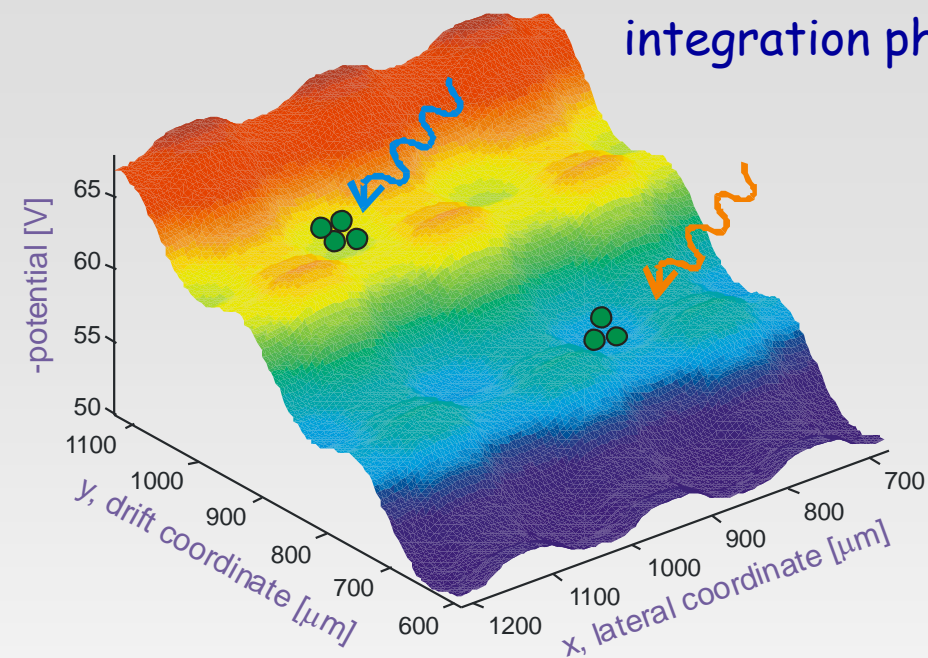
start-time and  
event-trigger  
(back side induction  
or ext. trigger)

stop-time and  
charge from  
anode signal





# MLSDD operating modalities - II



A. Castoldi, C. Guazzoni, C. Ozkan, G. Vedani, R. Hartmann and A. Bjeoumikhov, "Spectroscopic Imaging Applications", Microsc. Microanal. 15, 231-236, 2009

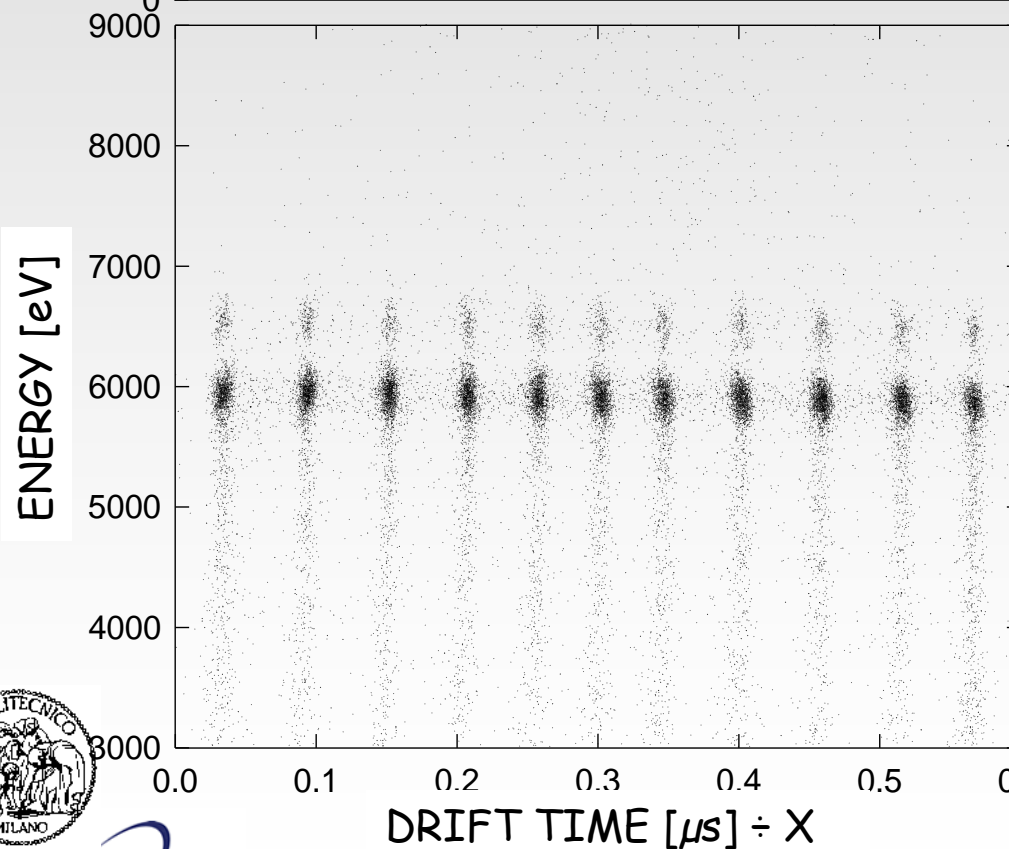
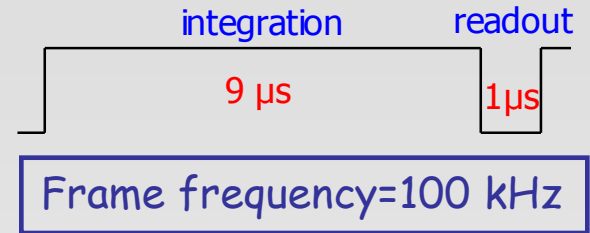
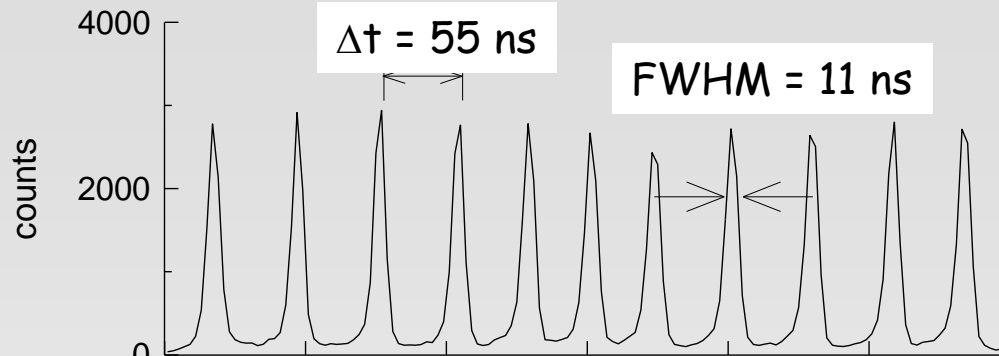
integrate-readout mode

Controlled-Drift Detector (1997)





# 1-D imaging & spectroscopy @100 kHz



Pixel  $180 \mu\text{m} \times 180 \mu\text{m}$

270 eV FWHM @ 300K @ 0.25  $\mu\text{s}$   
(28.6 el. r.m.s.)

198 eV FWHM @ 223K @ 0.5  $\mu\text{s}$   
(18.7 el. r.m.s.)

A.Castoldi, C.Guazzoni, P.Rehak, L.Strüder, et al,  
Trans. Nucl. Sci. 49 (3) June 2002

counts

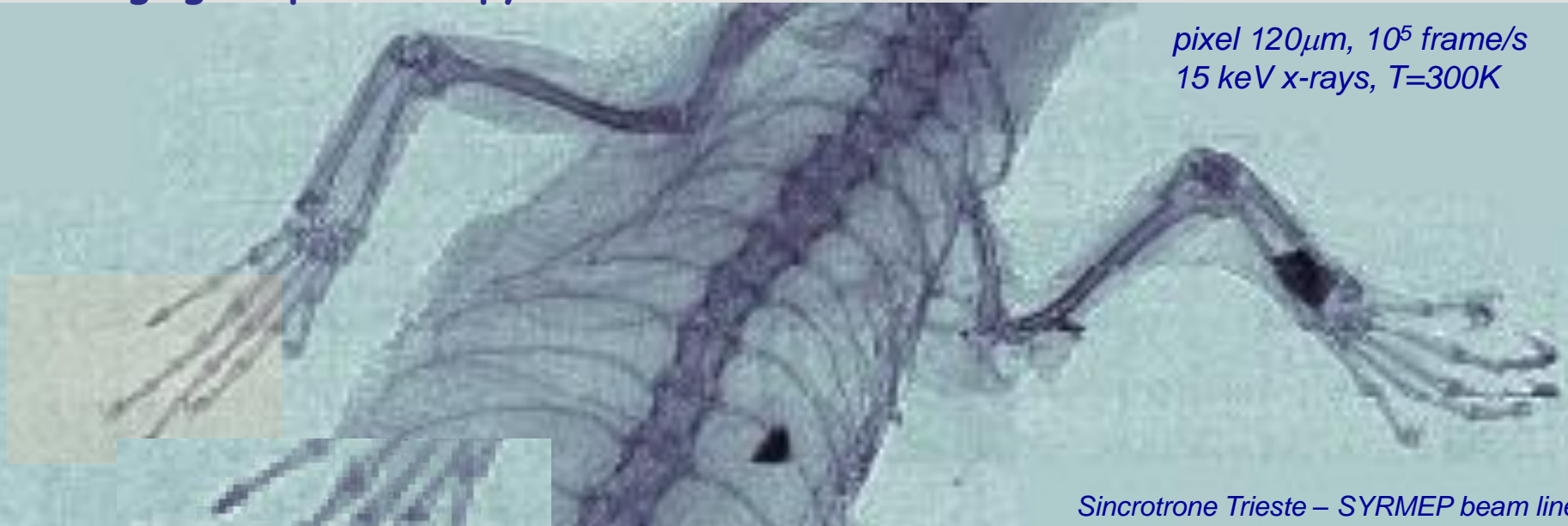


# 2-D spectroscopic X-ray imaging with CDDs

Exp. CODERA (2003)  
INFN - Sez. di Milano

2D imaging & spectroscopy

pixel  $120\mu\text{m}$ ,  $10^5$  frame/s  
15 keV x-rays,  $T=300\text{K}$



\* no animal was killed or suffered for this measurement

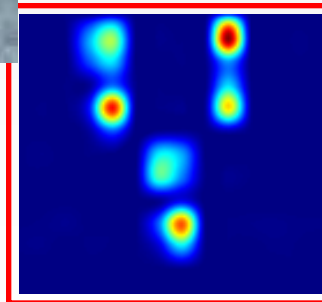
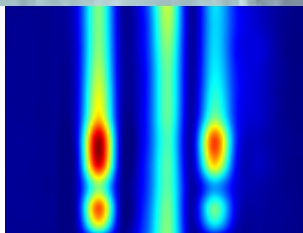
Sincrotrone Trieste – SYRMEP beam line

A.Castoldi, G. Cattaneo, A.Galimberti, C.Guazzoni, P.Rehak, L.Ströder, IEEE TNS 49, 3 (2002)

A.Castoldi, A.Galimberti, C.Guazzoni, P.Rehak, L.Ströder, NIM A512 (2003)

219 Hz sine wave  
Mask displacement:  
2.3 mm p-p

Time-s  
X-ray images



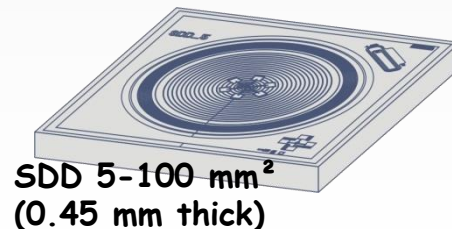
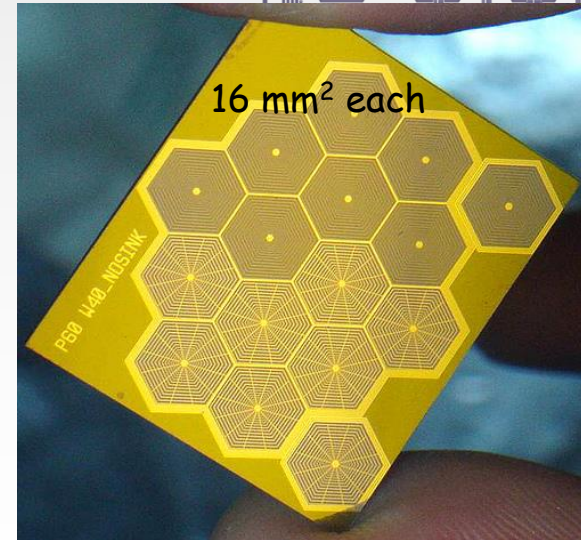
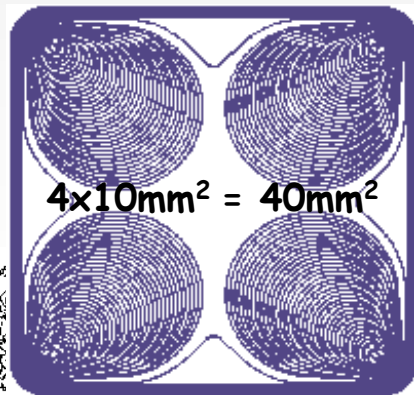
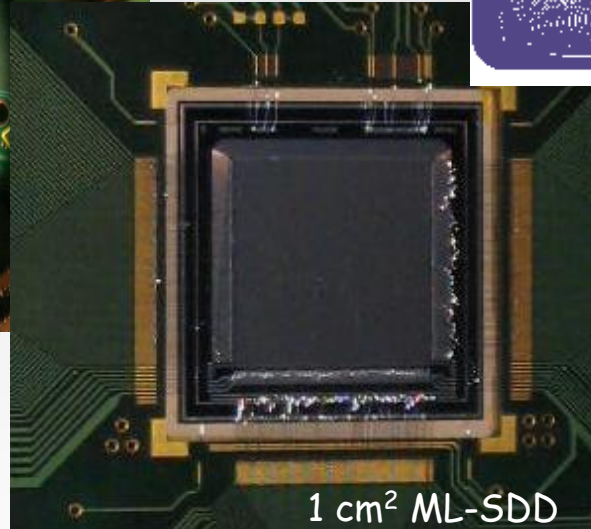
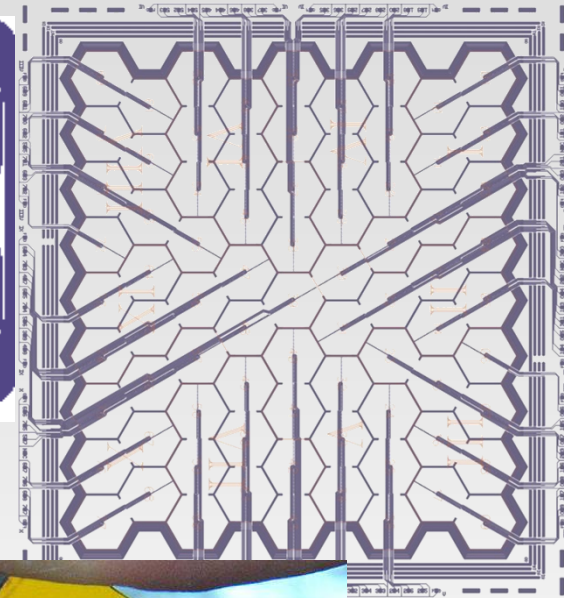
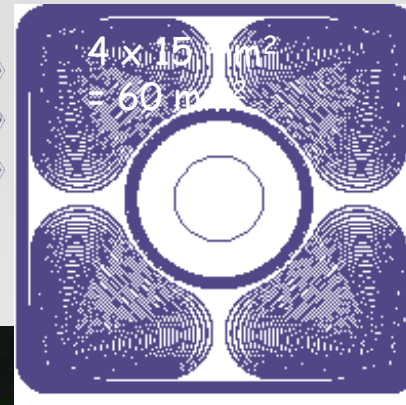
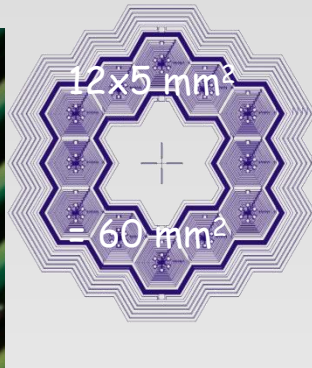
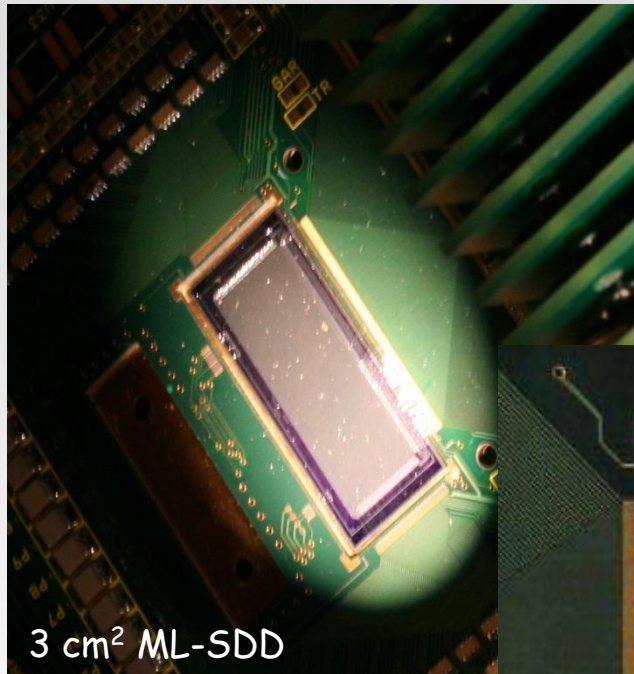
$\infty$

20  $\mu\text{s}$





# Outlook to applications...



# Outlook to applications...

☒ X-Ray Fluorescence and Proton Induced X-Ray Emission

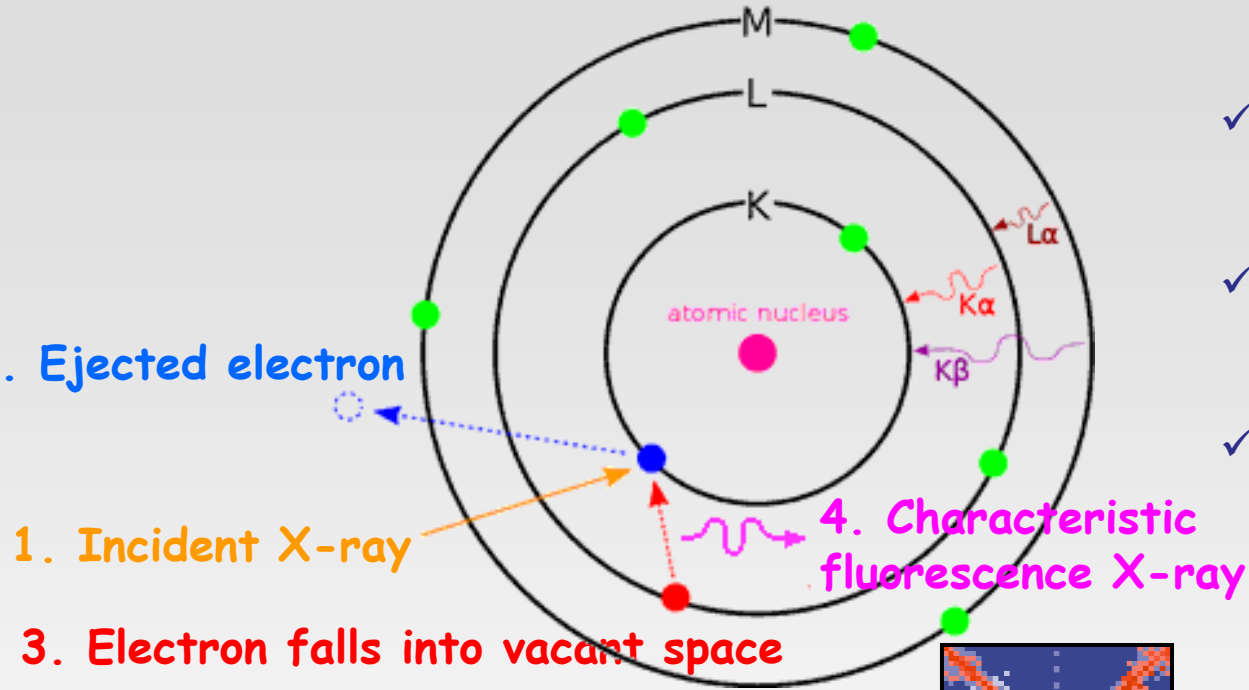
☐ Gamma-ray imaging

☐ Advanced X-ray imaging modalities

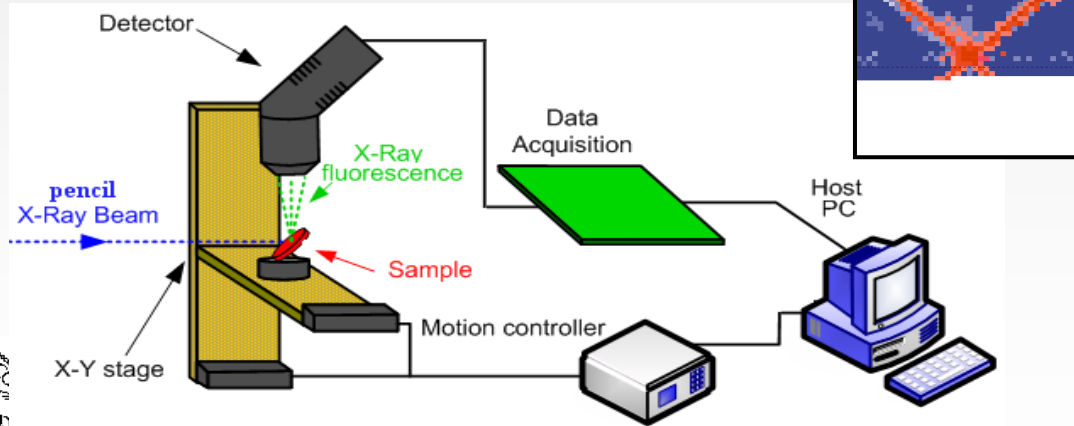
☐ Macro-pixel arrays with DEPFET readout for XFEL



# X-ray fluorescence imaging



- ✓ Energy of XRF X-ray is characteristic of element present in sample.
- ✓ Intensity of XRF signal is related to concentration of element in sample
- ✓ XRF is non-destructive.

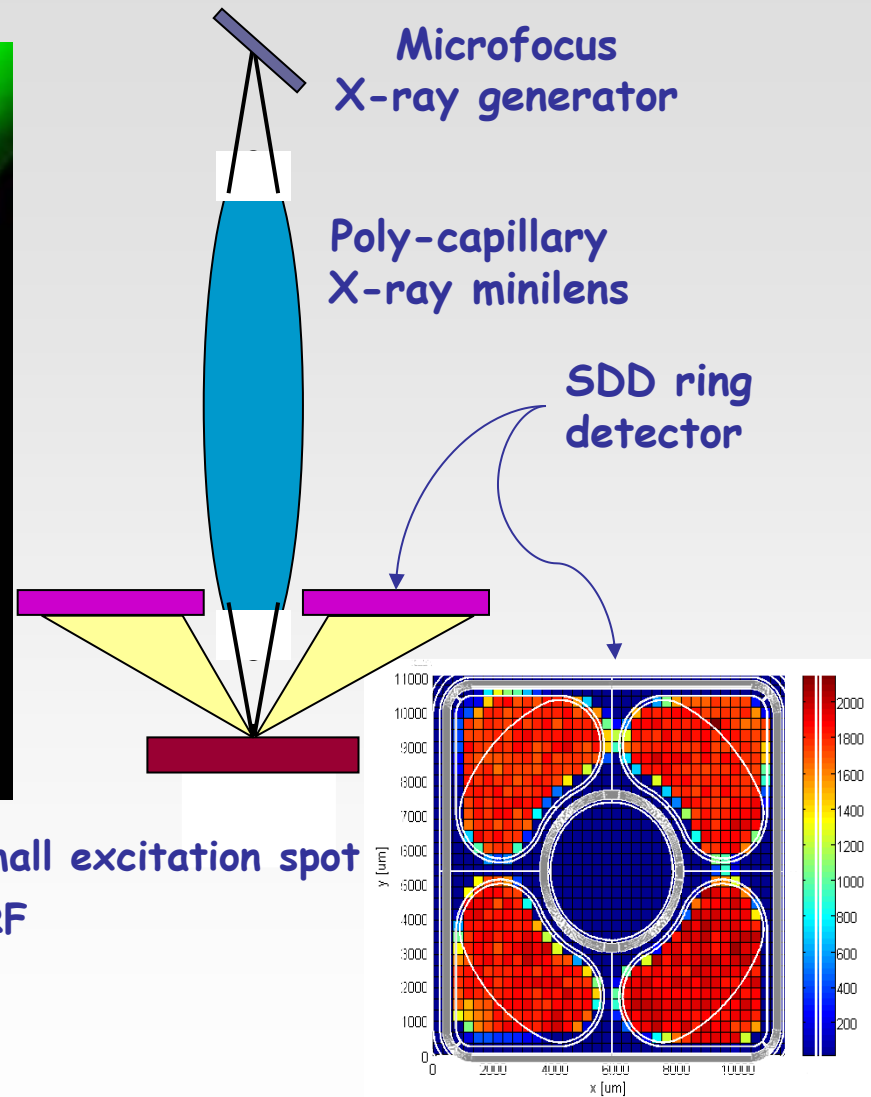
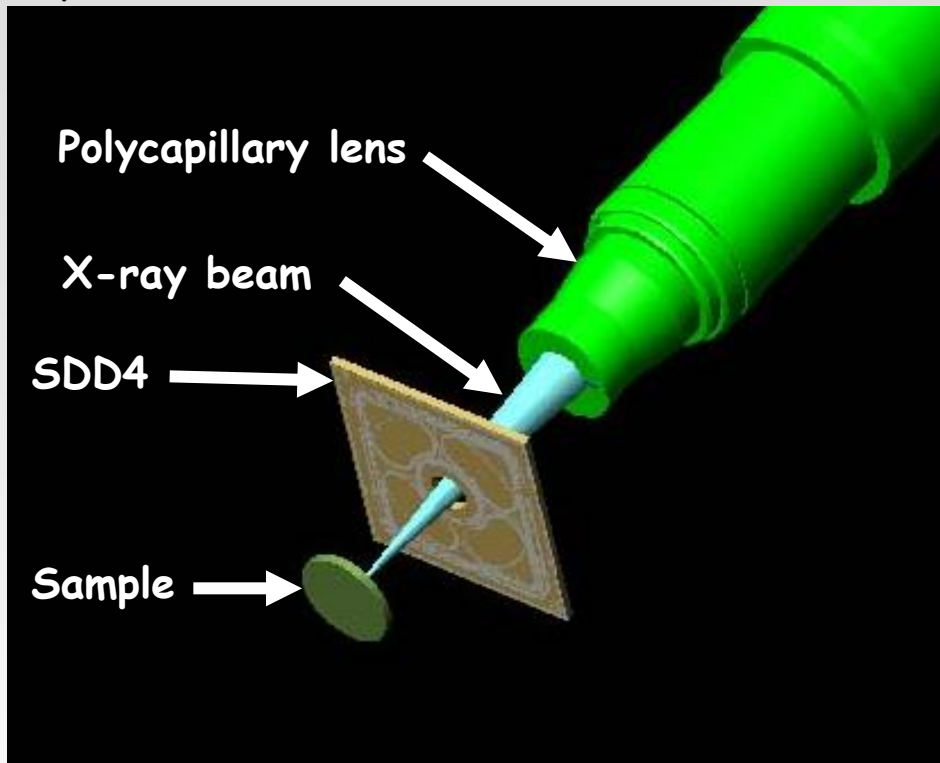


Usually technique performed by a 2D positional scan of a sample against a collimated beam with an energy dispersive detector.



# XRF elemental mapping with multi-cell SDDs

Experiment **FELIX** INFN Gr.5 2002-05

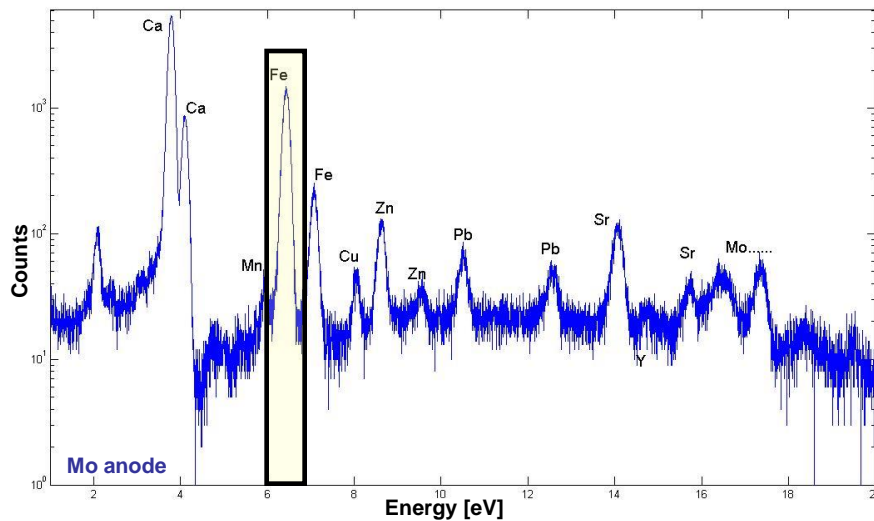
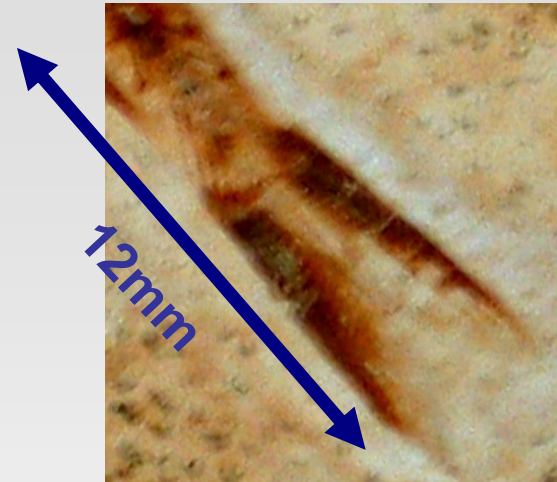
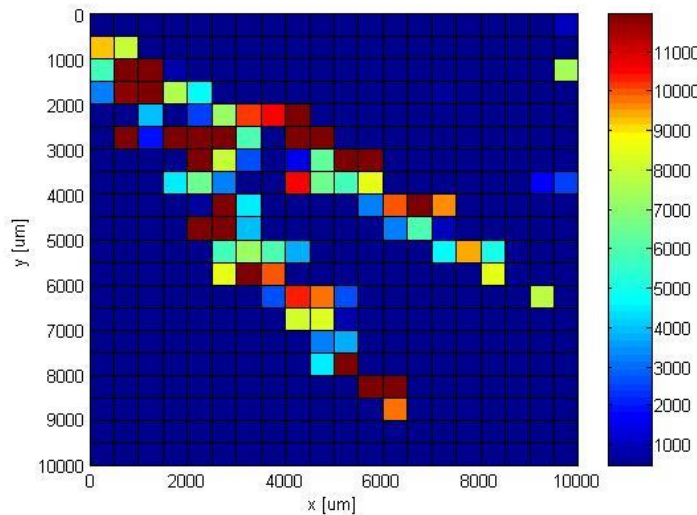


- polycapillary X-ray lens  $\rightarrow$  high photon flux in small excitation spot
- ring-shaped SDD  $\rightarrow$  larger collection angle of XRF





# Geological analyses: fossil fish



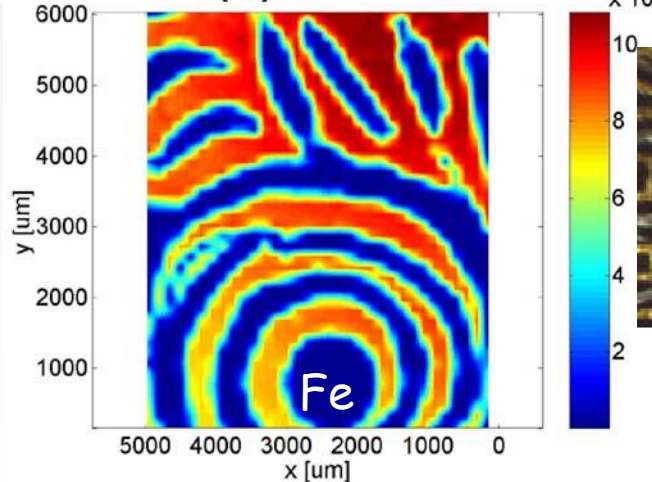
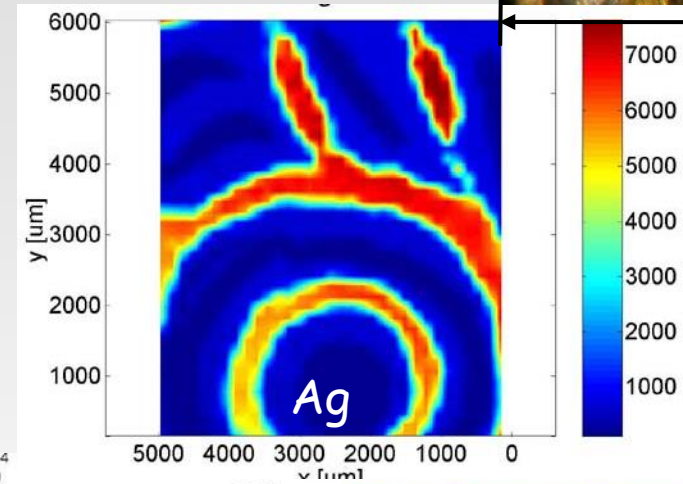
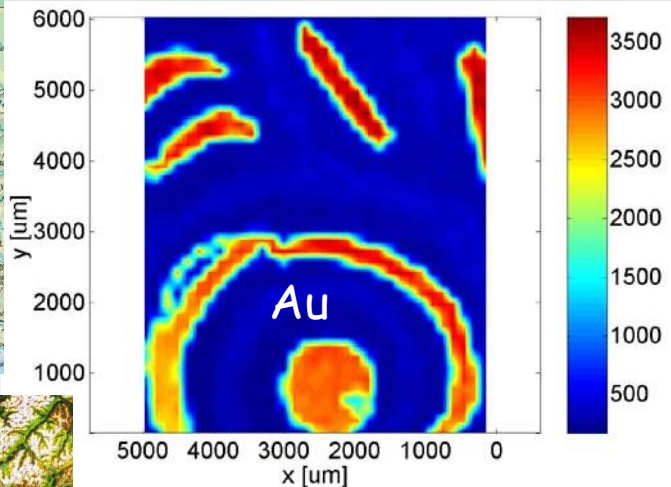
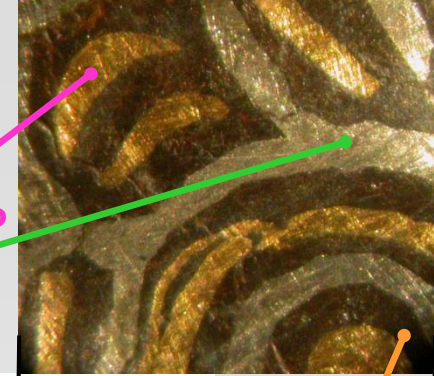
Map of Fe  $K\alpha$  line @ 6.4keV  
10x10mm with 500 $\mu$ m step  
2 sec per point  
Total meas. time 900sec

A. Longoni, C. Fiorini, C. Guazzoni, et al., Proc. of the IEEE 2005 NSS, Puerto Rico

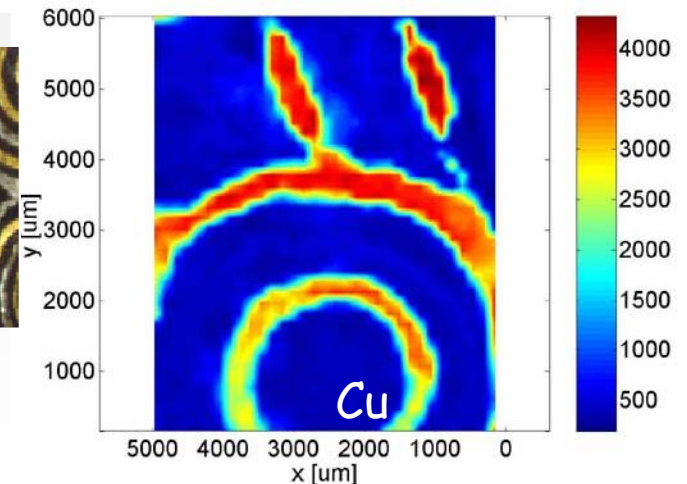
C. Guazzoni - Development of Silicon Drift Detectors and recent applications - Nov. 12, 2013  
2013 Workshop of the Technology and Innovation Group of the European Physical Society  
"Advanced Radiation Detectors for Industrial Use"

# Works of art

Lombard buckle - inlaid work (agemina) - Au ~97%  
beginning of VII century A.C. -  
Trezzo d'Adda, Italy  
Ag+Cu ~90%+7%



5 mm



~3 mm

Fe

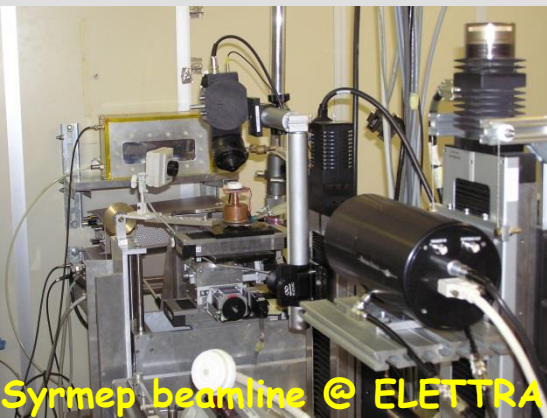
# XRF biomedical applications with SDDs

- ❑ study of the distribution of drugs and diagnostic agents in biological samples
  - in collaboration with Centro Studi Fegato, University of Trieste, Bracco Centro Ricerche Milano, Center of Molecular Biomedicine (Ts)
  - measurements @ SYRMEP beamline - ELETTRA SINCROTRONE Trieste, Italy
  
- ❑ theranostic imaging of tumours labelled with gold nanoparticles
  - in collaboration with Dept. of Medical Physics and Bioengineering, UCL, Division of Surgery and Interventional Science, UCL Medical School, IfG GmbH
  - measurements @ DIAMOND Beamline B16, Didcot, UK and in our lab - Polimi&INFN, Milano, Italy

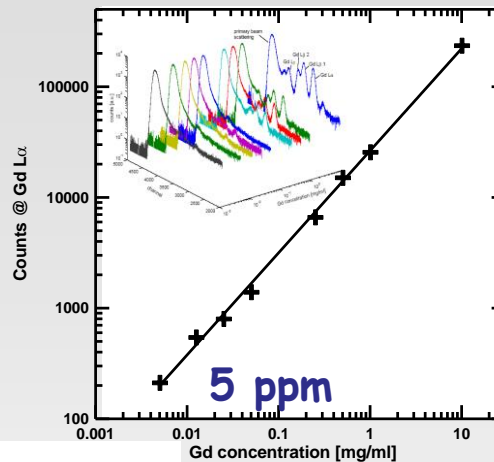




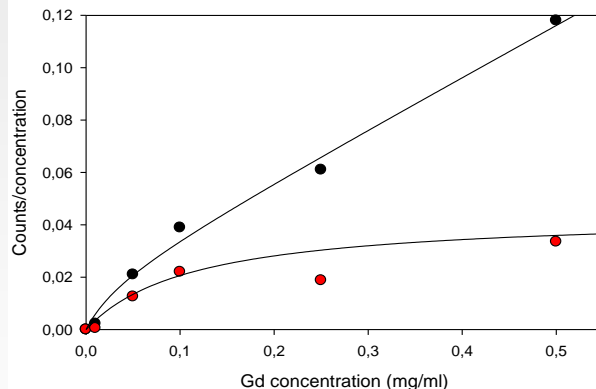
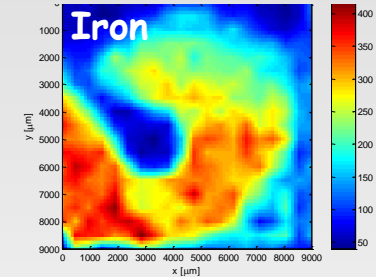
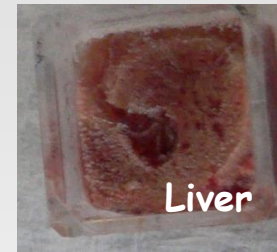
# Drugs and diagnostic agents distribution in biological samples



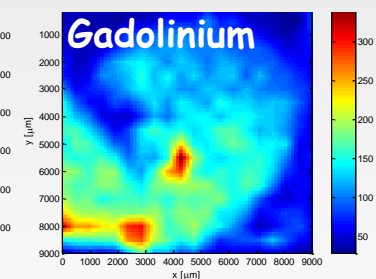
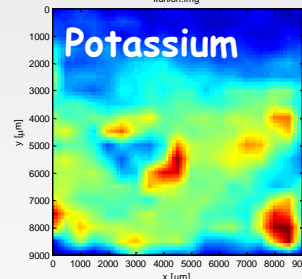
Gadolinium calibr. curve



hepatic uptake of Gadocoletic acid trisodium salt (B22956) agent



Scanned area:  
9mm x 9mm  
Step:  
500μm x 500μm.  
Measurement  
time: 60 s/point



→ no Gadolinium is detected in spleen, kidney and lung

$y = N_s \cdot x + (V_{max} \cdot x) / (K_m + x)$   $K_m = 0.0960 \pm 0.0339$  mg/ml  
of the same order of magnitude  
of the value assessed with  
radioactive markers

$N_s$  = nonspecific binding  
 $V_{max}$  = max velocity  
 $K_m$  = enzyme/substrate affinity

R. Alberti, C. Fiorini, C. Guazzoni, T. Klatka, A. Longoni, R. Delfino, V. Lorusso, L. Pascolo, L. Vaccari, F. Arfelli, L. Mancini, R. H. Menk, L. Rigon, G. Tromba, IEEE Nuclear Science Symposium Conference Records, 2006 IEEE, San Diego, California, Oct. 29 - Nov. 4, 2006 - Vol. 3, pp. 1528-1532

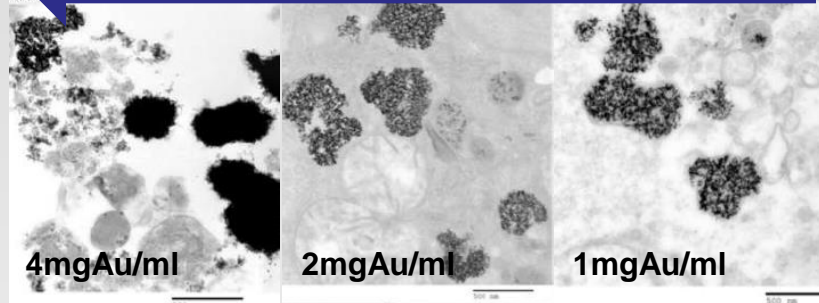
C. Guazzoni - Development of Silicon Drift Detectors and recent applications - Nov. 12, 2013  
2013 Workshop of the Technology and Innovation Group of the European Physical Society  
"Advanced Radiation Detectors for Industrial Use"





# Theranostic imaging of tumours labelled with gold nanoparticles

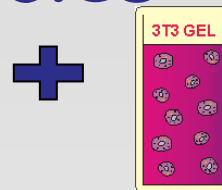
GNP concentration



TEM images of GNP-filled vesicles in HT29 cells incubated at different GNP concentrations



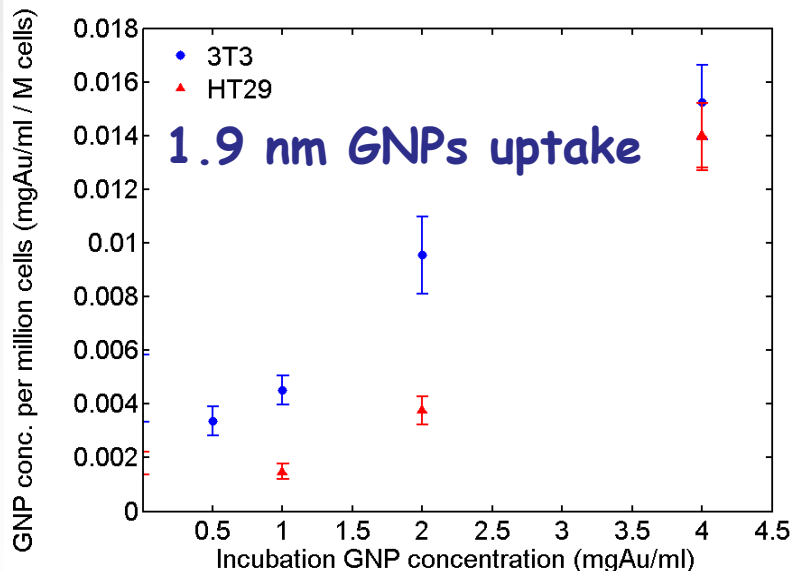
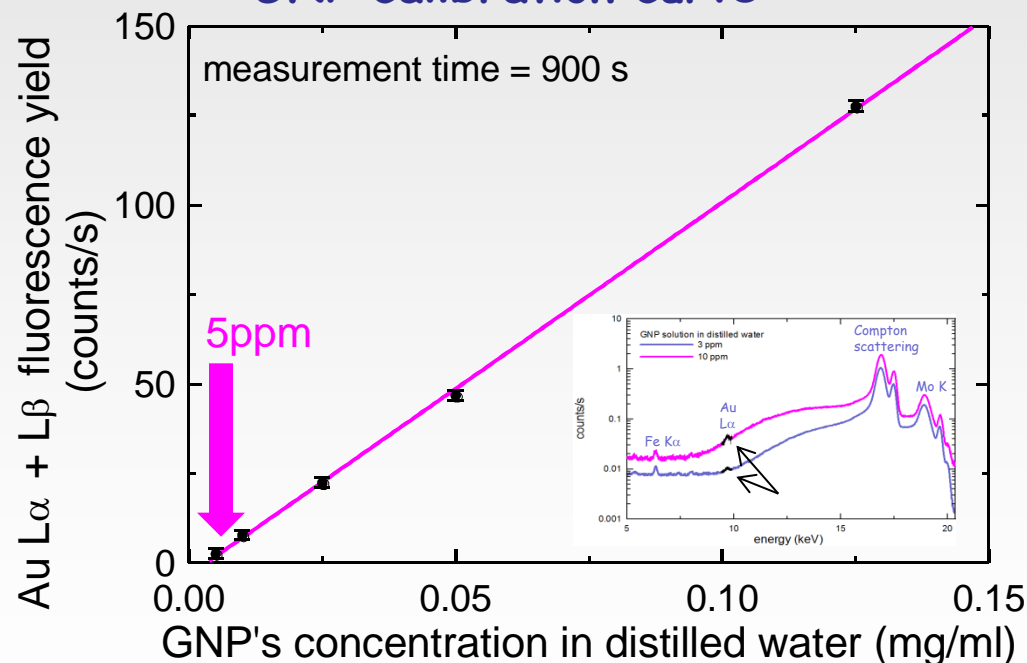
artificial cancer mass of HT29 cells with GNP inclusions



non-dense collagen gel populated by 3T3 fibroblasts



## GNP calibration curve



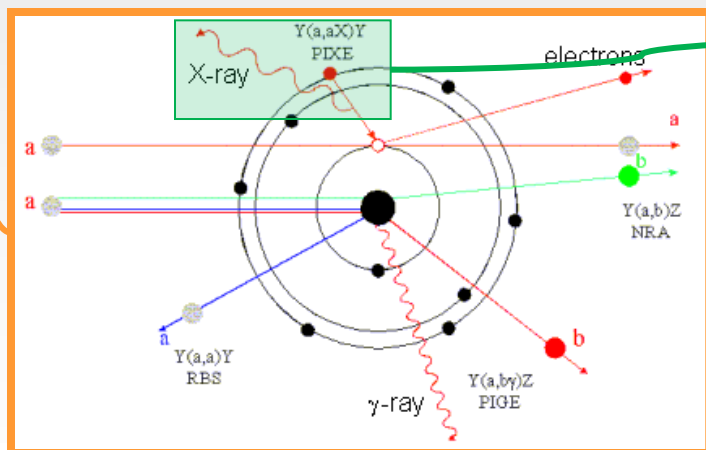
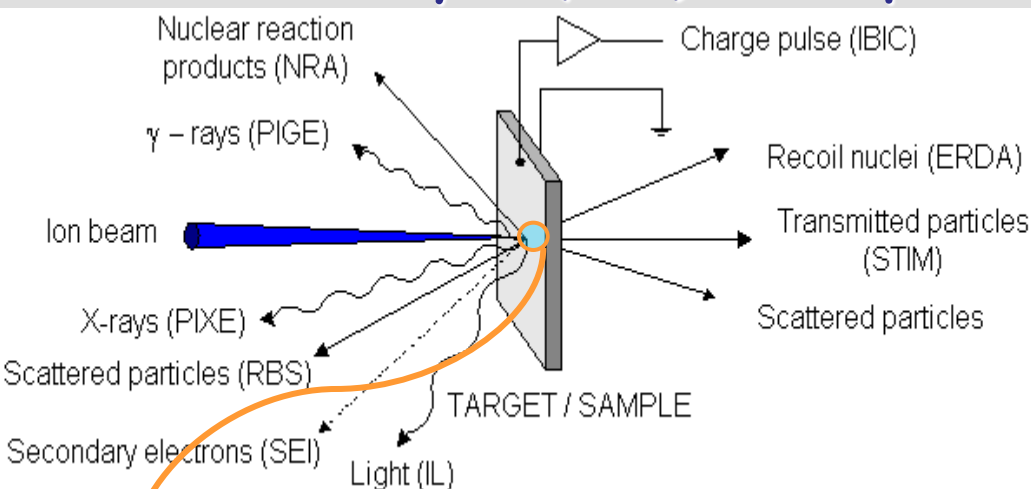
minimum detection limit: 3 ppm

C. Guazzoni - Development of Silicon Drift Detectors and recent applications - Nov. 12, 2013  
2013 Workshop of the Technology and Innovation Group of the European Physical Society  
"Advanced Radiation Detectors for Industrial Use"

K. Ricketts, C. Guazzoni, A. Castoldi, A. P. Gibson and G. J. Royle, *Phys. Med. Biol.*, vol. 58, 2013, pp. 7841-7856,

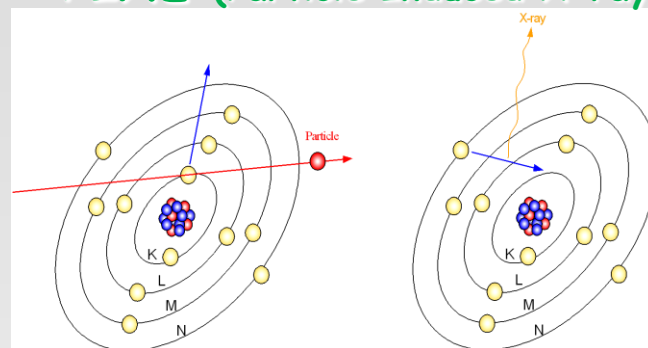
# IBA techniques and PIXE

## Ion Beam Analysis (IBA) techniques



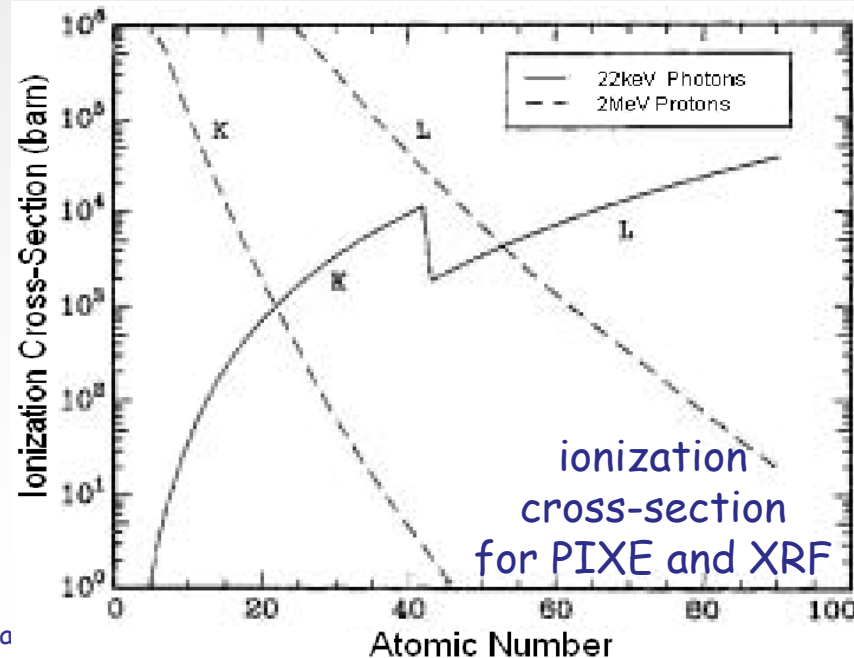
- sample as target of beam of accelerated particles with energy of the order of few MeV.
- secondary radiation energy is characteristic of the emitting atom or nucleus.

## PIXE (Particle Induced X-ray Emission)



ionization  
process

- Multi-elemental
- Quantitative
- Non-destructive

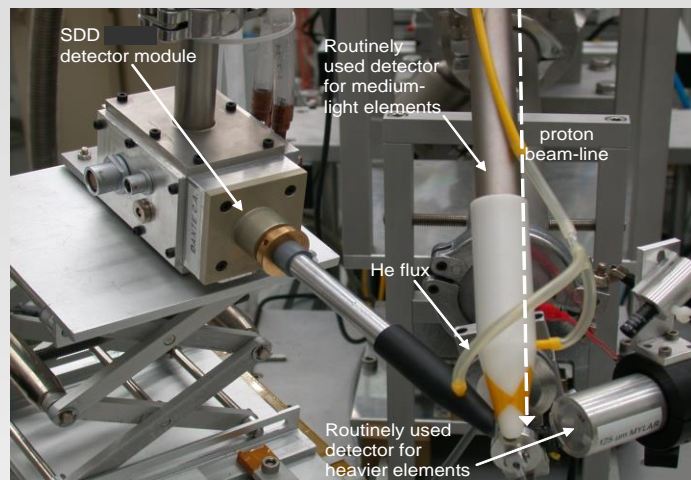


ionization  
cross-section  
for PIXE and XRF



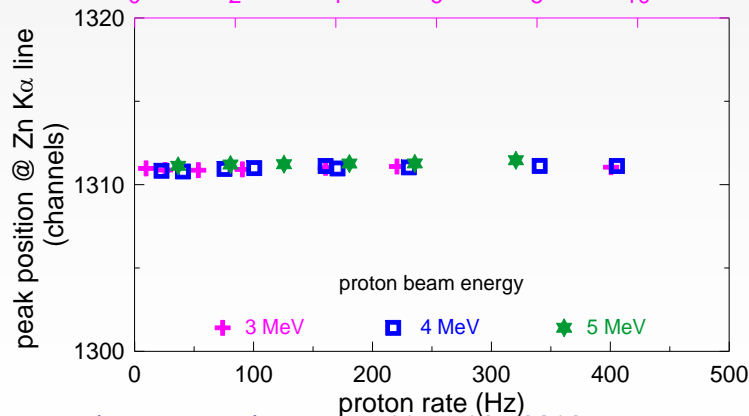
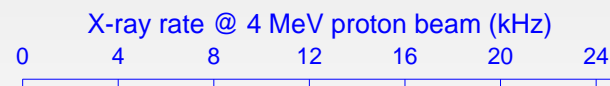
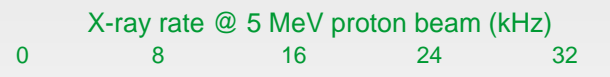
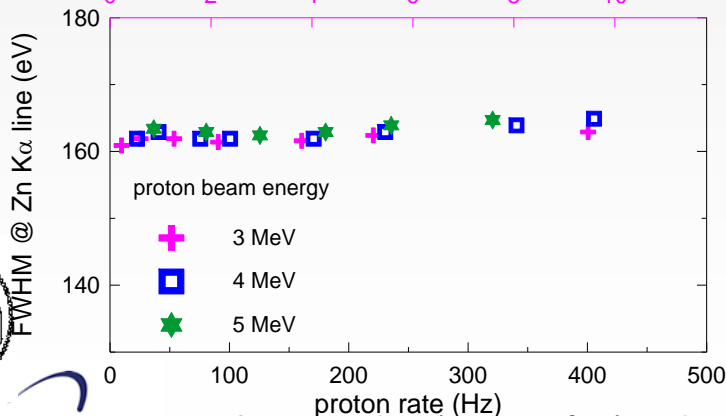
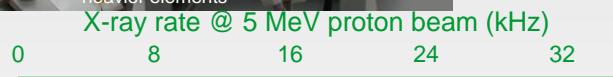
# SDD-based PIXE setup - 1

Esp. DANTE  
INFN Gr.5 2006-08  
Labec, INFN Firenze



- advantages of SDDs in count rate and energy resolution
- problem: at low X energies (medium-light elements) back-scattered particles degrade energy spectra even at low particle rates

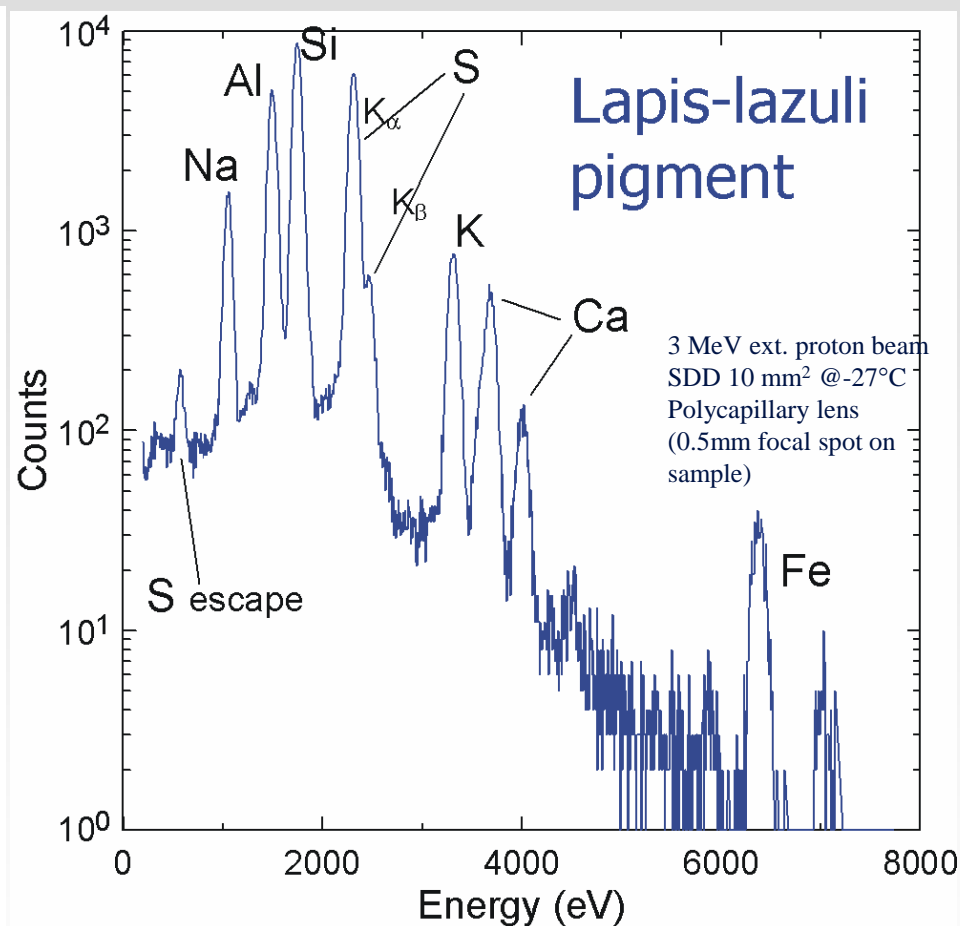
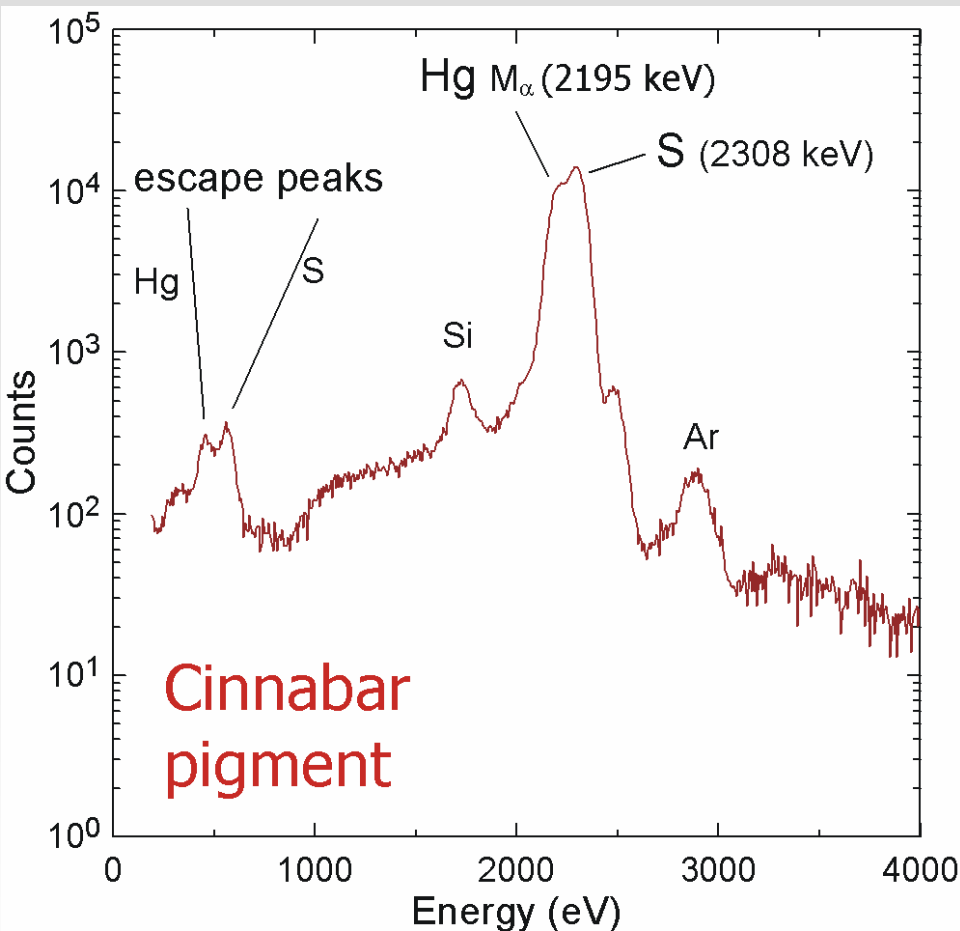
→ SDD+customized front-end electronics with optimized pulsed reset able to manage the large-signal of particle events without degradation



C. Guazzoni - Development of Silicon Drift Detectors and recent applications - Nov. 12, 2013  
2013 Workshop of the Technology and Innovation Group of the European Physical Society  
"Advanced Radiation Detectors for Industrial Use"

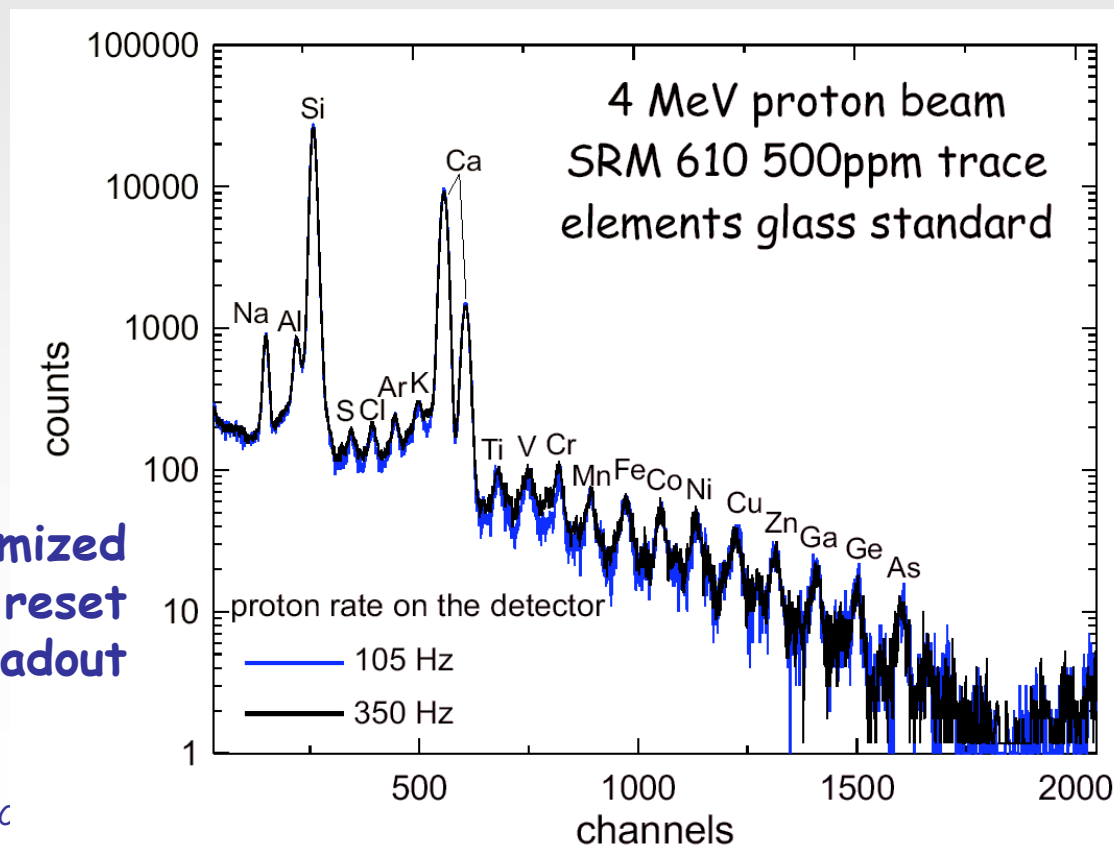
R. Alberti, N. Grassi,  
C. Guazzoni, T. Klatka, NIM A  
607 (2009) 458-462

# SDD-based PIXE setup - 2





# SDD-based PIXE setup - 2



with optimized  
pulsed reset  
readout



# Outlook to applications...

□ X-Ray Fluorescence and Proton Induced X-Ray Emission

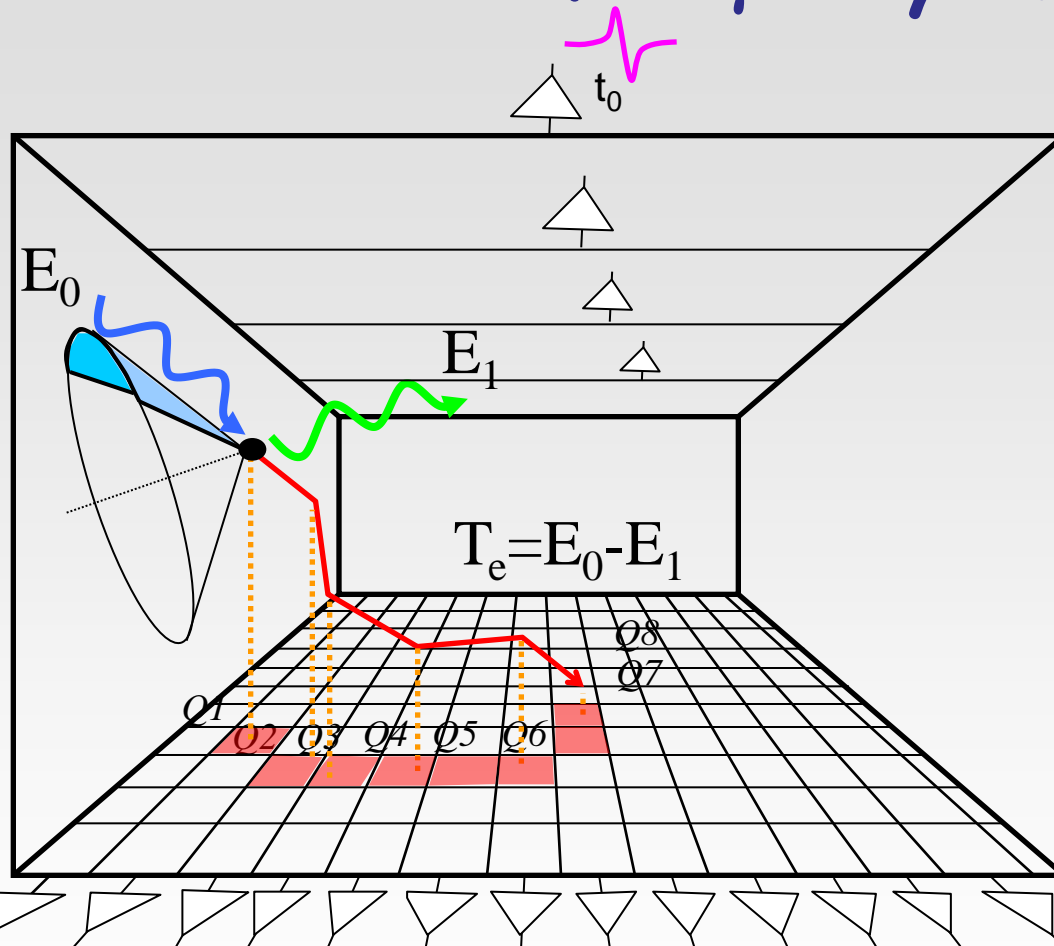
□ Gamma-ray imaging

□ Advanced X-ray imaging modalities

□ Macro-pixel arrays with DEPFET readout for XFEL



# High-resolution Compton scatter detector for $\gamma$ -ray imaging



interaction time given from fast induction signal on back strips

→ *fast coincidence imaging in Compton telescope arrangement*

electron tracking with high spatial and energy resolution

→ *vertex of the interaction*

→ *initial direction of recoil electron*

(reduction multiple Coulomb scattering issue)

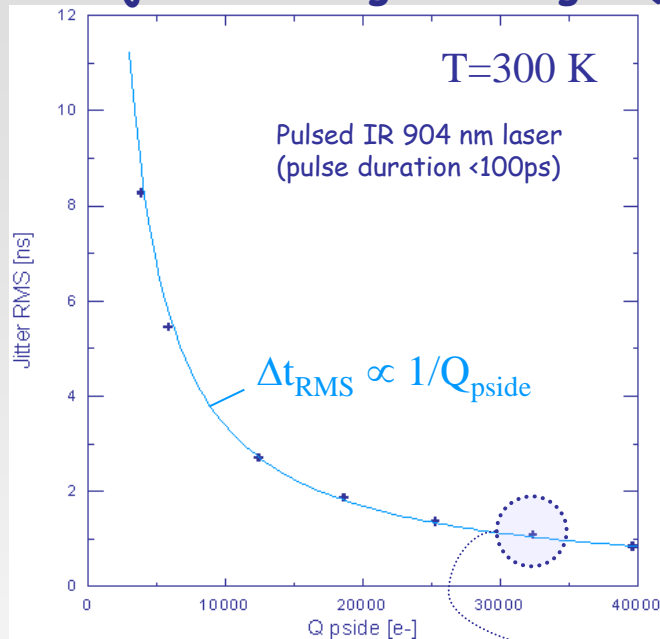
→ *estimate of  $dE/dx$*

*Silicon MLSDD scatter detector  
with readout of backside strips*

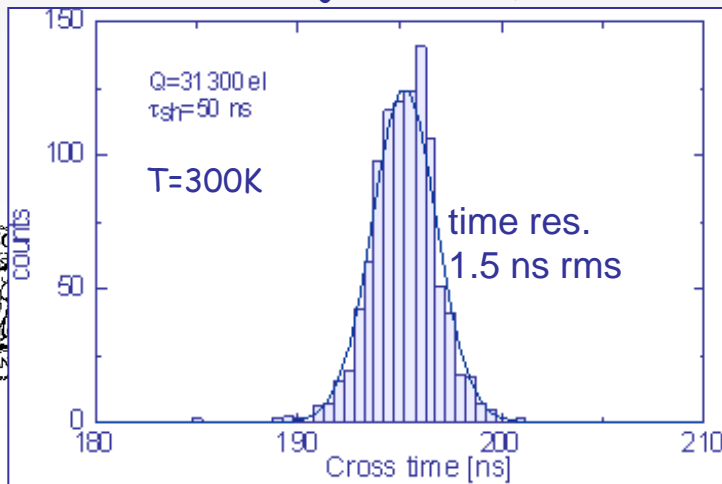


# Timing resolution

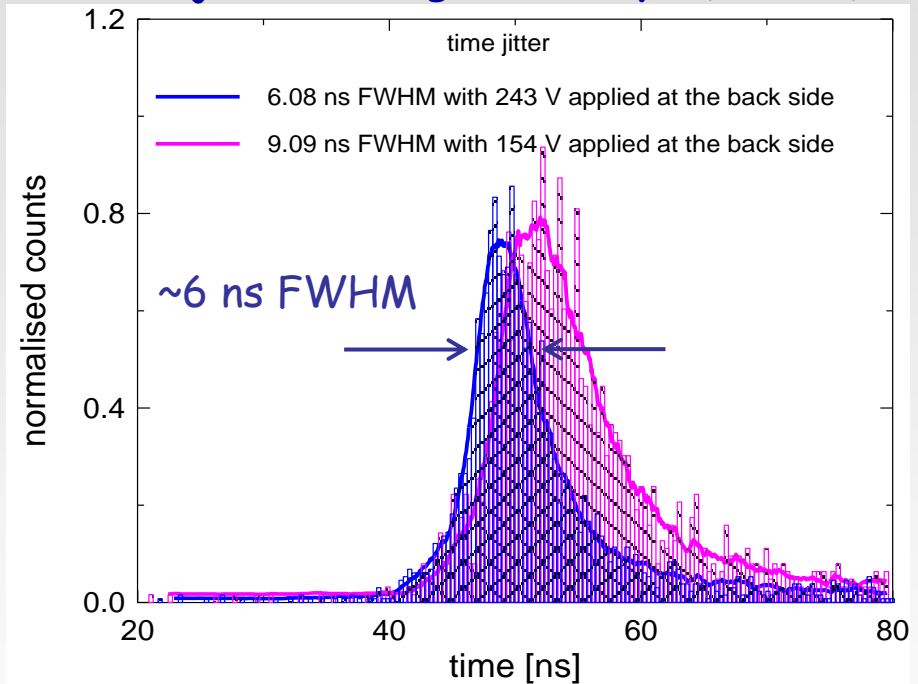
## Time jitter vs. signal charge Q



## Measured time jitter @ $Q=31300$ el



## Time jitter with gamma-rays (Na-22)



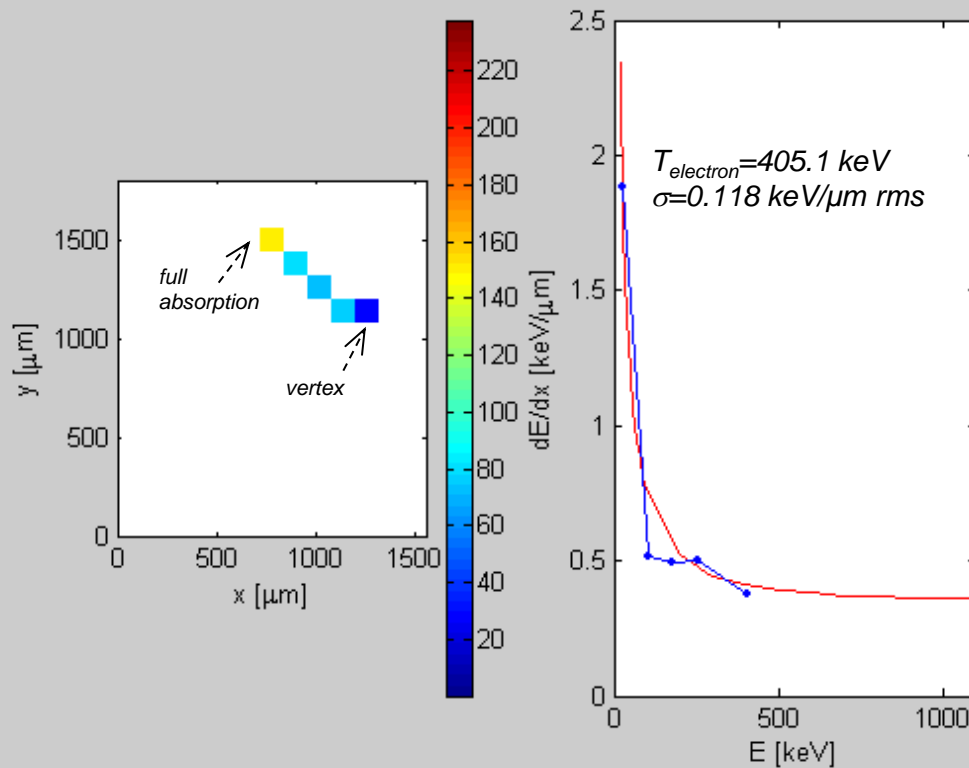
A.Castoldi, E.Gatti, C.Guazzoni, Nucl. Instr. and Meth. A518 (2004) 429-432

Opens to coincidence imaging  
with  $\sim 10\text{ ns rms}$  time resolution



# Electron tracks

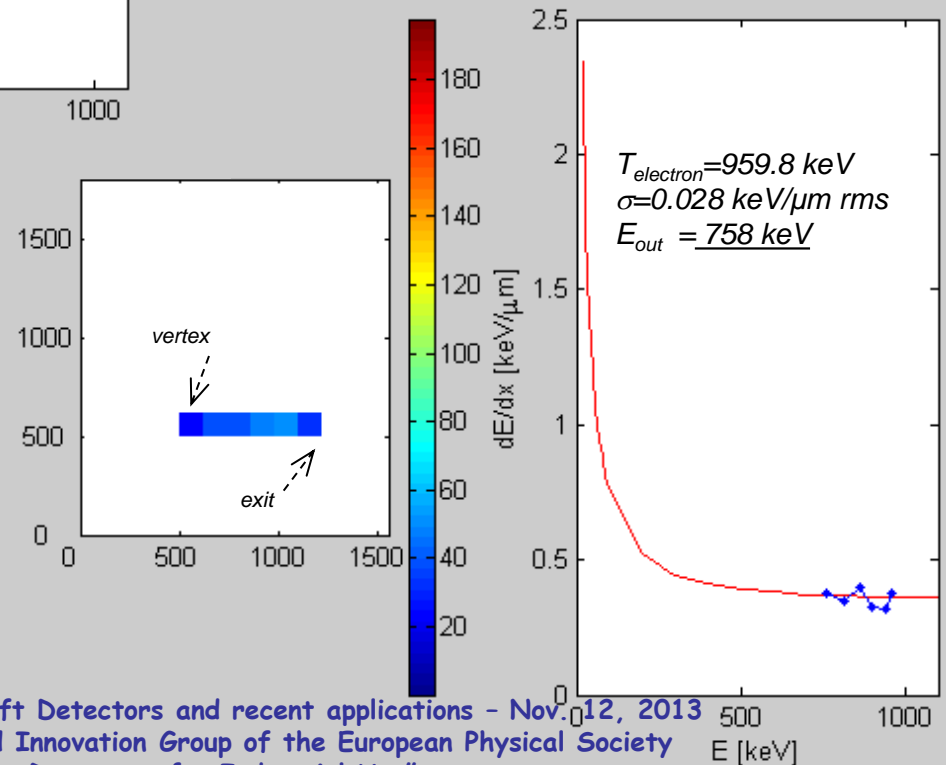
Na-22 source, T=300K



*Z-exit*

*internal absorption*

1-st experimental evidence of electron tracks resolved in space and energy in a single silicon layer



A. Castoldi, A. Galimberti, C. Guazzoni, P. Rehak, R. Hartmann, L. Ströder, Nucl. Instr. and Meth. A 568 (2006) 89-95

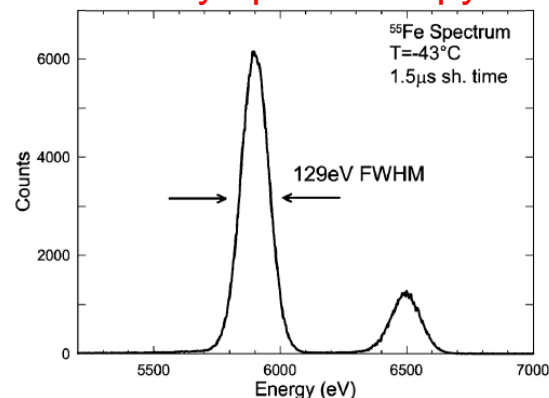
C. Guazzoni - Development of Silicon Drift Detectors and recent applications - Nov. 12, 2013  
2013 Workshop of the Technology and Innovation Group of the European Physical Society  
"Advanced Radiation Detectors for Industrial Use"



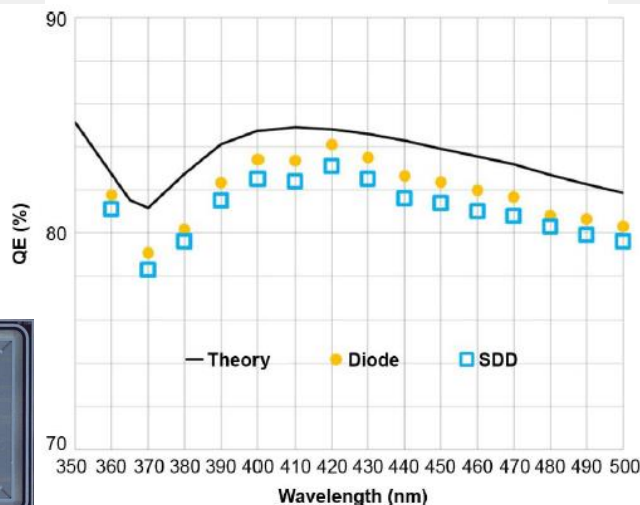
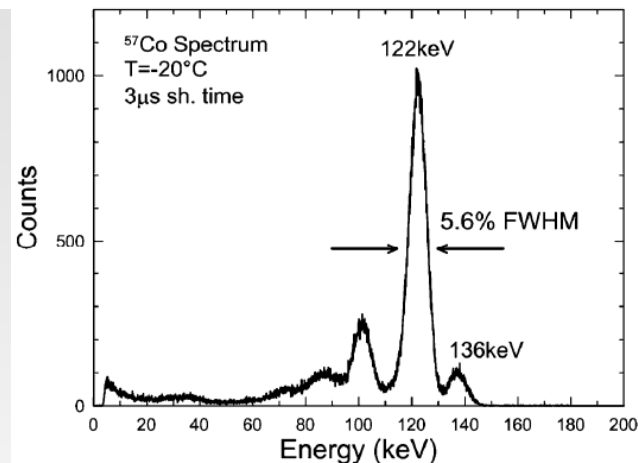
# Silicon Drift Detectors for Readout of Scintillators in Gamma-Ray Spectroscopy

Carlo Fiorini, Luca Bombelli, Paolo Busca, Alessandro Marone, Roberta Peloso, Riccardo Quaglia,  
 Pierluigi Bellutti, Maurizio Boscadin, Francesco Ficorella, Gabriele Giacomini, Antonino Picciotto,  
 Claudio Piemonte, Nicola Zorzi, Nick Nelms, and Brian Shortt

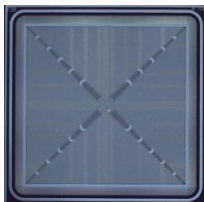
## X-ray spectroscopy



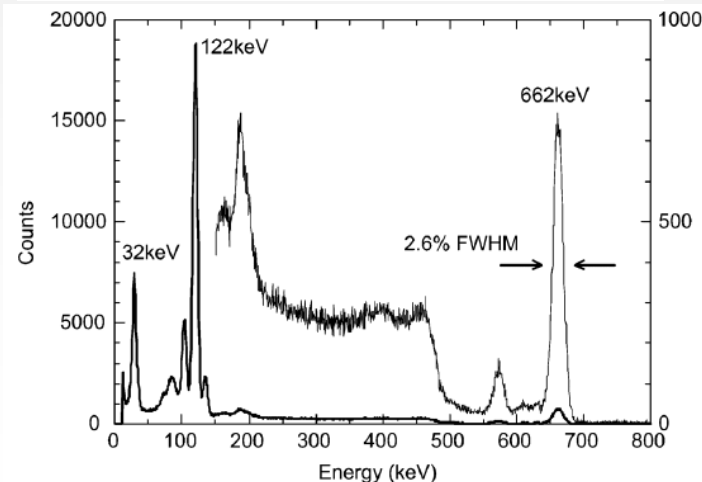
## γ-ray spectroscopy with LaBr<sub>3</sub>



thin entrance  
 window suitable for  
 both soft X-ray  
 detection (>200 eV)  
 and scintillator  
 readout



area = 64 mm<sup>2</sup>



carlo.fiorini@polimi.it  
 Politecnico di Milano, Italy



# Outlook to applications...

□ X-Ray Fluorescence and Proton Induced X-Ray Emission

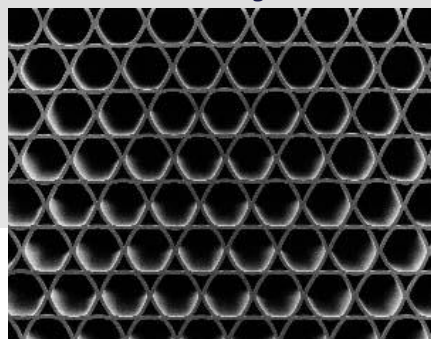
□ Gamma-ray imaging

□ Advanced X-ray imaging modalities

□ Macro-pixel arrays with DEPFET readout for XFEL

# X-ray Scatter Imaging (XSI)

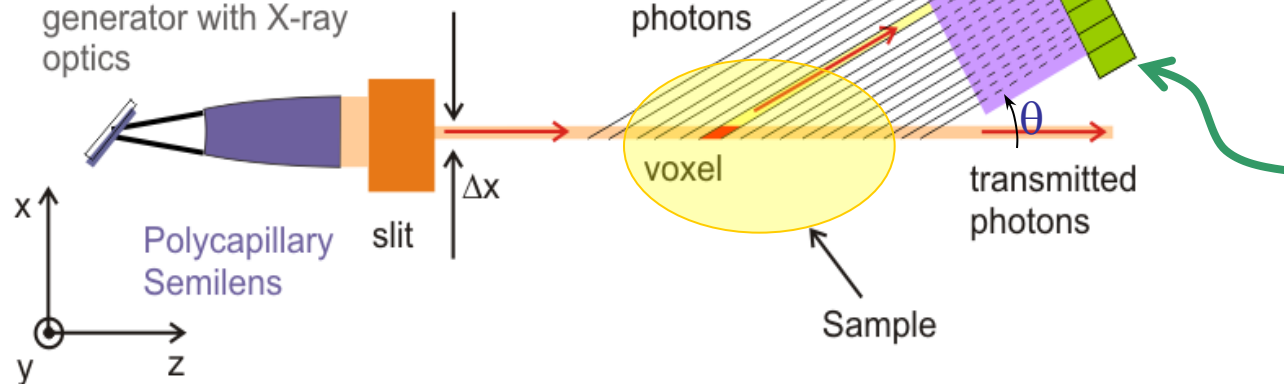
Polycapillary technology for beam collimation and angular selection



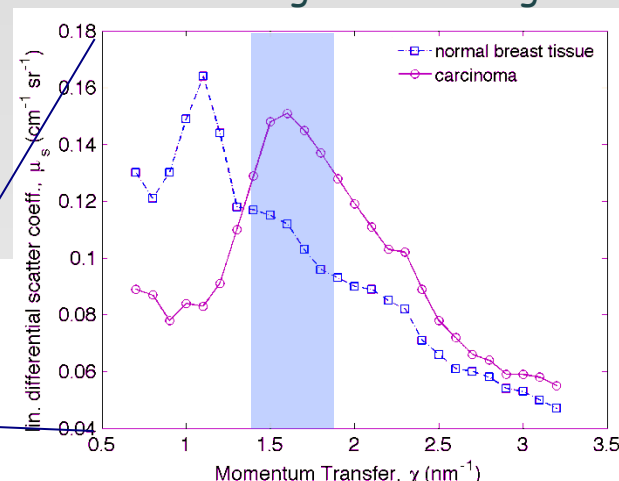
1-30 $\mu$ m

Parallel Polycapillary Collimator 1:1

conventional X-ray generator with X-ray optics



materials scatter X-rays at distinctive angles and energies



$$\chi = E/hc * \sin(\theta/2)$$

Controlled Drift Detector as 2D imager with high spectroscopic resolution

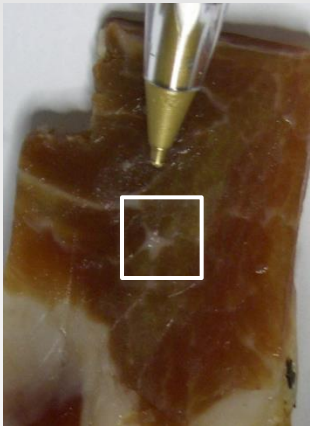
- ✧ Polycapillary technology allows full exploitation of detector pixel resolution
- ✧ 2D spectroscopic imager (Controlled Drift Detector) allows imaging at multi-momentum transfer values





# Scatter images vs TX images with standard collimation @ Synchrotron ELETTRA

*pork sample with  
2mm detail*

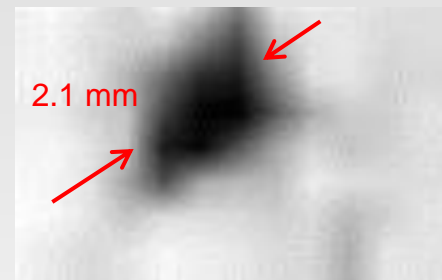


Transmission image  
(pixel 180 $\mu$ m)

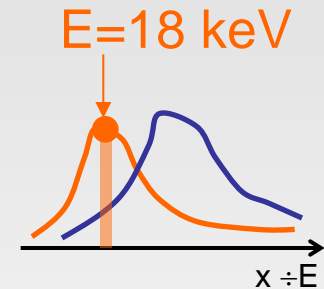


contrast=33%

Scatter image  
(pixel 500 $\mu$ m)



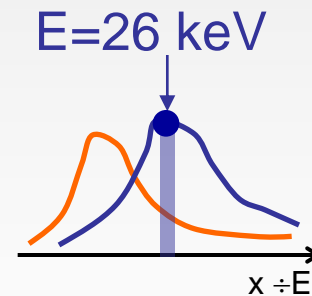
contrast=46%



contrast=11%



contrast=29%



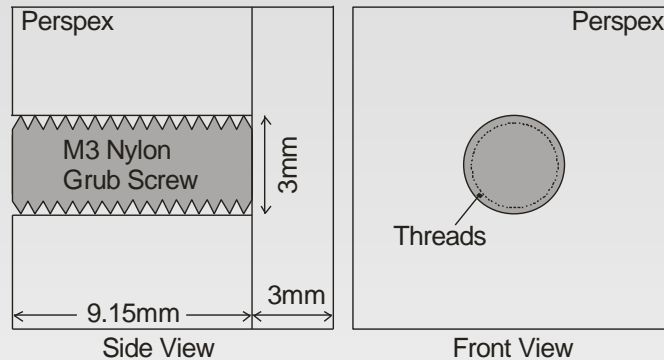
A. Castoldi, C. Guazzoni, A. Galimberti,  
R. Hartmann, S. Pani, G. Royle, and L.  
Strüder, IEEE Trans. Nucl. Sci. 54  
(2007) pp. 1474-1480

- contrast optimization with energy selection
- conventional mechanical collimation limits spatial resolution

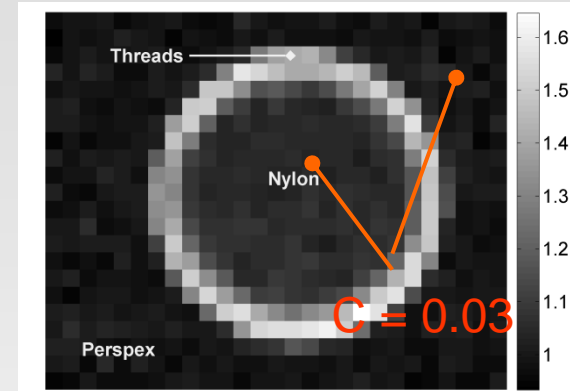


# X-ray Scatter imaging with X-ray tube and high-resolution polycapillary collimation

Perspex / Nylon6,6 Phantom

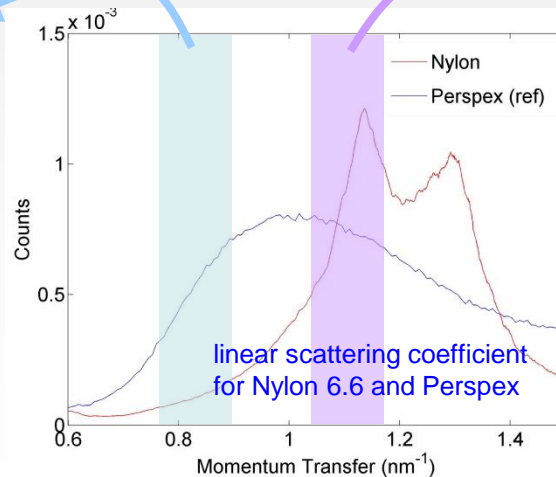
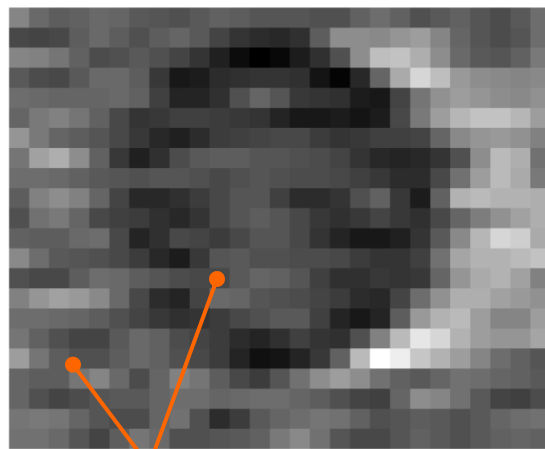


Transmission

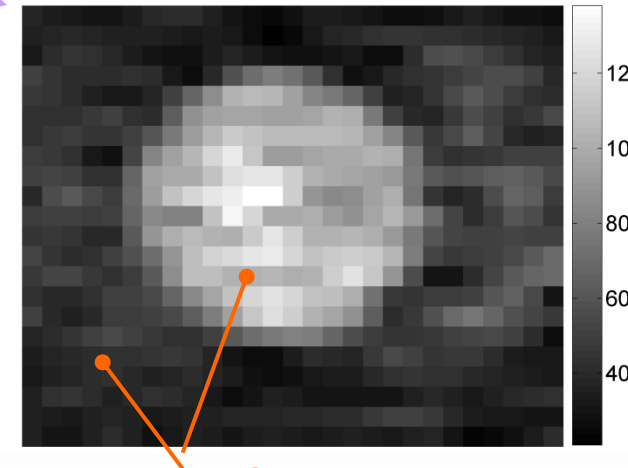


## Multi-momentum imaging (energy selection)

12-14keV



16.5-18.5keV



# Outlook to applications...

☐ X-Ray Fluorescence and Proton Induced X-Ray Emission

☐ Gamma-ray imaging

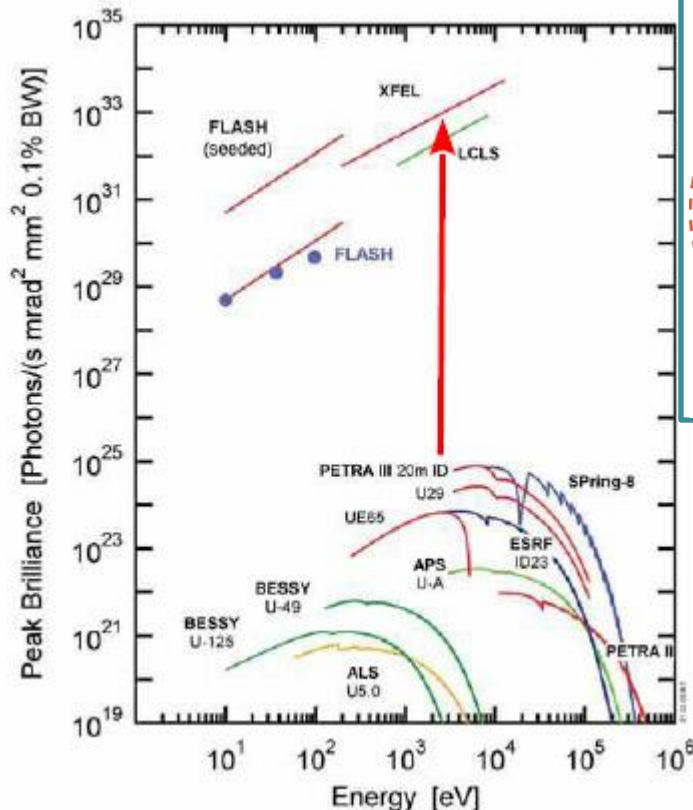
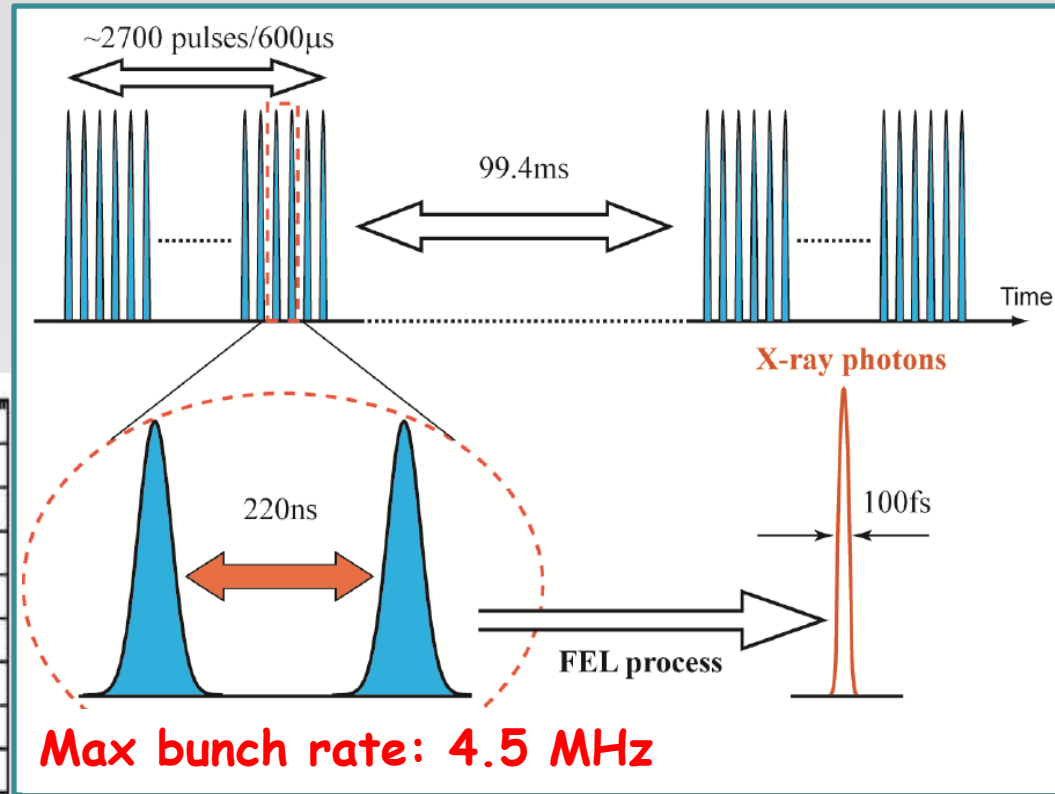
☐ Advanced X-ray imaging modalities

☐ Macro-pixel arrays with DEPFET readout for XFEL



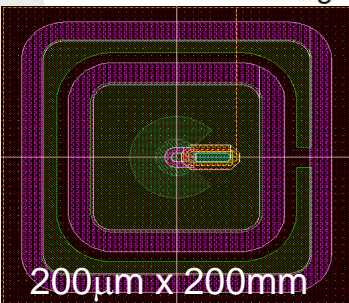
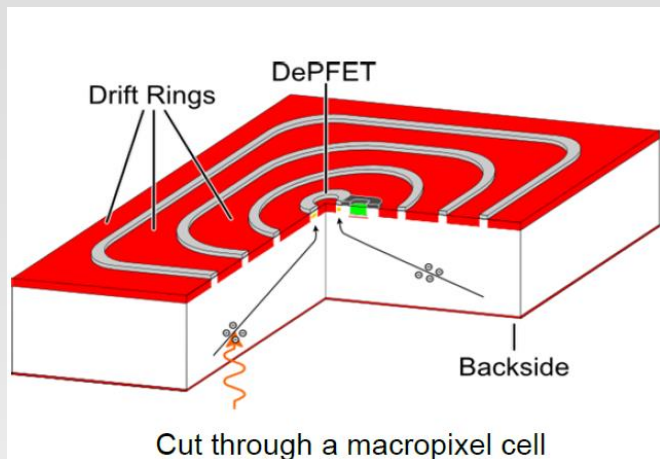
# 2D area detectors for XFEL beams

scheduled for  
operation end  
2015



- ✓ high dynamic range ( $<10^4$  X-rays/pixel)
- ✓ high speed ( $\sim 5$  Mframes/s)
- ✓ low noise ( $E=2-15$  keV)

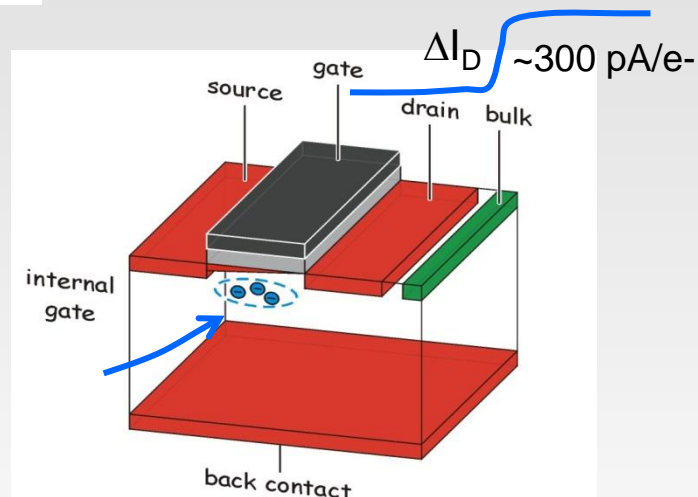




consortium

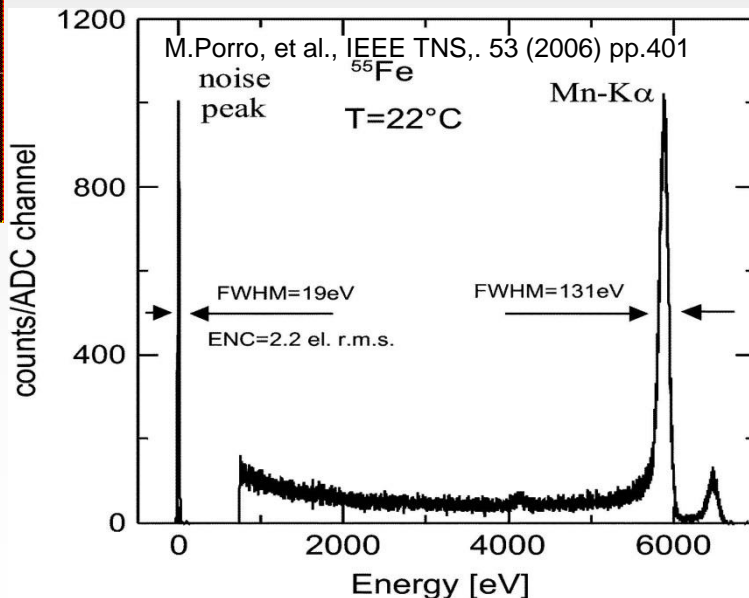


**PN**Sensor



- Drift structure to allow fast and complete collection at buried gate
- DEPFET readout

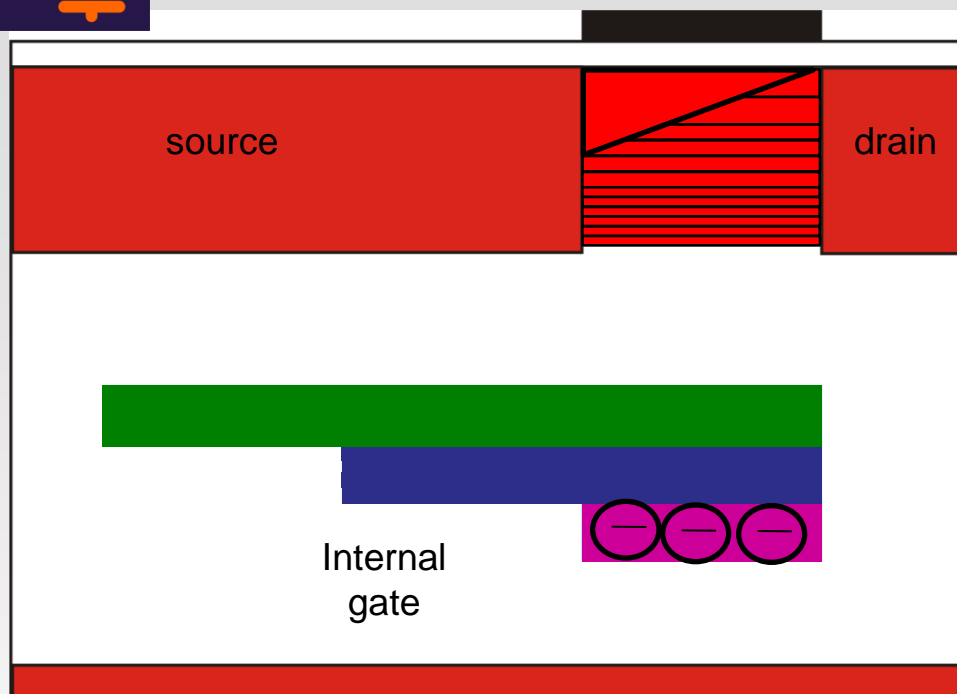
- ✓ collecting anode=internal gate
- ✓ high energy resolution (2 keV photon counting)
- ✓ analog compression



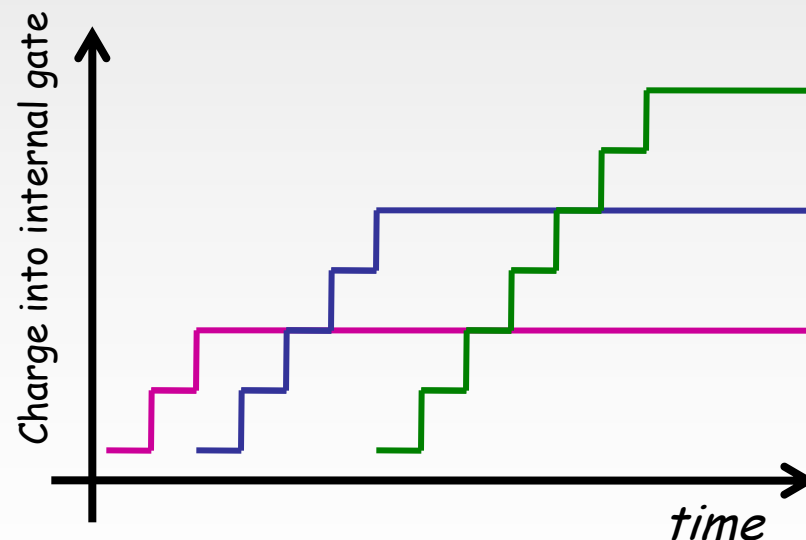
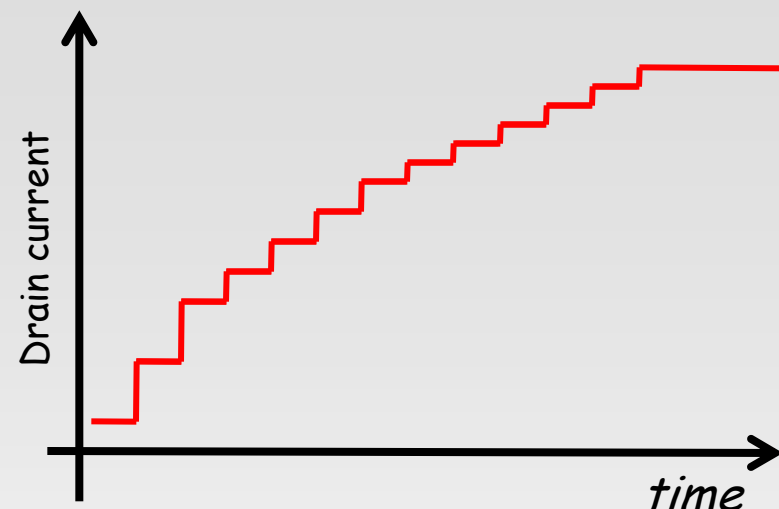
M.Porro, et al.  
IEEE Trans. Nucl.  
Sci., Vol. 59, 2012,  
pp. 3339 - 3351



# DEPFET with signal compression



- ✓ The internal gate extends into the region below the source
- ✓ Small signals assemble below the channel, being fully effective in steering the transistor current
- ✓ Large signals spill over into the region below the source. They are less effective in steering the transistor current.

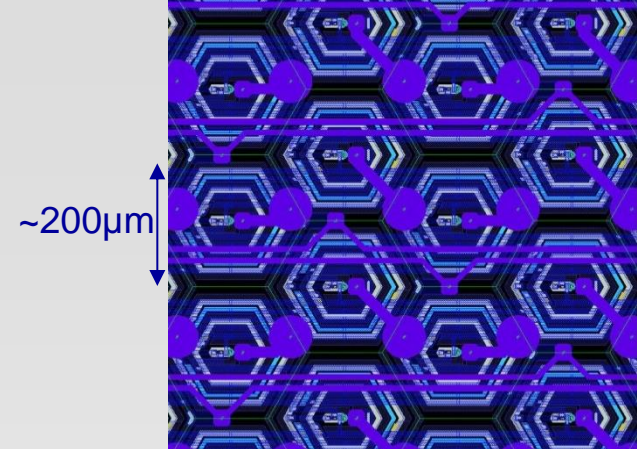
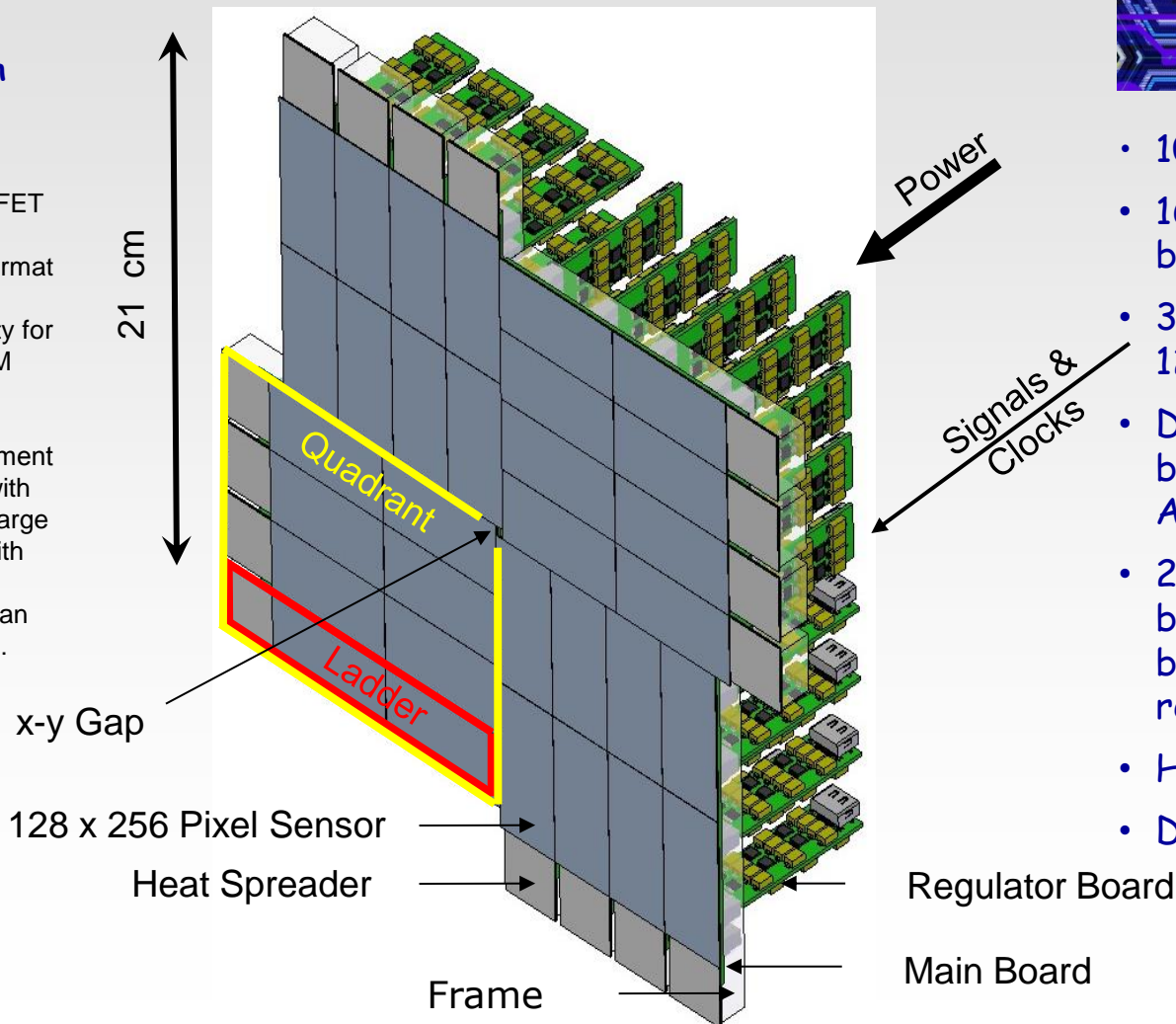


# DSSC Focal plane overview

Developed by DSSC consortium  
(Italy-Germany)  
under contract with  
DESY/XFEL GmbH

M. Porro et al., "Expected Performance of the DEPFET Sensor with Signal compression: a Large Format X-ray Imager with Mega-Frame Readout Capability for the European XFEL", NIM A624 (2010) 509

M. Porro et al., "Development of the DEPFET Sensor with Signal Compression: a Large Format X-Ray Imager With Mega-Frame Readout Capability for the European XFEL", IEEE Trans. Nucl. Sci. 59 (2012) 3339



- 1024x 1024 pixels
- 16 ladders/hybrid boards
- 32 monolithic sensors 128x256 6.3x3 cm<sup>2</sup>
- DEPFET Sensor bump bonded to 8 Readout ASICs (64x64 pixels)
- 2 DEPFET sensors wire bonded to a hybrid board connected to regulator modules
- Heat spreader
- Dead area: ~15%

Regulator Board

Main Board

# Conclusions

- ❑ **Silicon Drift Detectors** were **invented** by E. Gatti and P. Rehak **almost 30 years ago** as particle-tracking detectors in physics experiment.
- ❑ Nowadays **widely spread in X-ray spectroscopy**, and **commercially available** in different shapes and sizes
- ❑ **Conventional and non-conventional applications** have been shown (e.g., nondestructive analysis of cultural heritage, environmental monitoring, industrial control based on XRF and XRD, novel diagnostic tools for biomedical imaging with X and gamma-rays, etc.).
- ❑ As Gatti and Rehak stated in their first patent, “**additional objects and advantages of the invention** will become **apparent to those skilled in the art**”

Let us hope to be skilled enough in the art to reach new milestones in this fascinating field and keep “drifting” on towards new horizons...





Thank you for your attention...

*...and a special thank to everyone  
who actively contributed  
in this exciting development*